

CT Evaluation of the Myocardial Blood Supply: Dual-Source Dual-Energy CT

Sung Min Ko

Contents

1	Introduction	80
2	Principles of Material Decomposition in Dual-Energy CT	80
3	Configuration of Dual-Source Dual-Energy CT	81
3.1	First Generation Dual-Source Dual-Energy CT (Siemens Definition).....	81
3.2	Second Generation Dual-Source Dual-Energy CT (Siemens Definition Flash).....	81
4	Methodology for Dual-Energy CT Image Acquisition	82
4.1	Image Acquisition of Rest Dual-Energy CT.....	82
4.2	Image Acquisition of Stress Dual-Energy CT.....	83
4.3	Image Reconstruction of Dual-Energy CT.....	84
4.4	Post-Processing, Display, and Analysis.....	84
5	Overview of Imaging Modalities for Coronary Artery Disease	85
6	Overview of Single-Energy CT Perfusion Imaging	87
7	Dual-Energy CT Perfusion Imaging	89
7.1	Dual-Energy CT at Rest for Myocardial Perfusion.....	89
7.2	Dual-Energy CT Under Stress for Myocardial Perfusion....	92
7.3	Comparison Between Rest Dual-Energy CT and Stress Dual-Energy CT Perfusion Imaging.....	95
8	Challenges, Pitfalls, and Limitations of Dual-Energy CT Perfusion	97
8.1	Radiation Dose.....	97
8.2	Artifacts.....	98
9	Summary and Conclusion	99
	References	101

Abstract

With dual-source CT in dual-energy mode, two X-ray tubes are operated independently at different voltages, acquiring two data sets showing different attenuation levels. An “iodine distribution map” is used for the assessment of myocardial blood pool status by analyzing iodine distribution within the myocardium based on the specific absorption characteristics of iodine for high and low X-ray energy spectra. Contrast-enhanced dual-energy computed tomography (DECT) perfusion with the patient at rest enables the evaluation of changes in the status of the myocardial blood supply. Rest DECT iodine distribution maps make hypoperfused myocardium more conspicuous and assist in the identification of areas exhibiting reversible myocardial ischemia. Rest DECT has thus expanded the clinical application of multidetector CT, as a “one stop shop” imaging modality to identify both coronary artery disease and myocardial blood pool deficits in a single examination. Stress DECT perfusion has the potential to become a robust clinical tool for the detection of myocardial ischemia. The combined approach of coronary CT angiography and stress DECT perfusion allows identification of hemodynamically significant coronary lesions in high-risk patients with a large calcified plaque burden or stents. This chapter provides a protocol setup and the characteristic features of dual-source DECT, and derives its benefits and limitations for DECT myocardial perfusion.

Abbreviations

CAD	Coronary artery disease
CCA	Conventional coronary angiography
CCTA	Coronary computed tomography angiography
CT	Computed tomography
DECT	Dual-energy computed tomography
ECG	Electrocardiography
FFR	Fractional flow reserve

S. M. Ko (✉)
Department of Radiology,
Konkuk University Hospital,
Konkuk University School of Medicine,
Gwangjin-gu, Seoul, Korea
e-mail: ksm9723@yahoo.co.kr

HU	Hounsfield Unit
LV	Left ventricular
MDCT	Multidetector computed tomography
MPI	Myocardial perfusion imaging
MR	Magnetic resonance
SPECT	Single-photon emission computed tomography

1 Introduction

Dual-energy computed tomography (DECT) was initially introduced for the purpose of spectral differentiation of material through the utilization of two X-ray spectra; however, technical limitations have prevented the clinical application of this concept for more than two decades (Chiro et al. 1979; Millner et al. 1979). The advent of dual-source CT, with two acquisition systems (two X-ray tubes and two detector arrays) mounted in the same gantry and operated independently with respect to voltage and current settings, has allowed for the analysis of energy-dependent changes in the attenuation of different materials (Flohr et al. 2006; Johnson et al. 2007; Petersilka et al. 2008). The differentiation of iodine in tissue can be of clinical diagnostic value. In addition to the Hounsfield unit (HU) attenuation values, DECT perfusion provides further information based on the specific absorption characteristics of iodine for high- and low-energy X-rays, facilitating specific tissue characterization and mapping of the iodine distribution. This “iodine distribution map” depicts myocardial blood volume, or perfusion status. With this depiction, one can easily visualize blood pool deficits and detect hemodynamically significant coronary artery stenoses. Recently, several single-center studies applying DECT have reported a strong correlation with single-photon emission computed tomography (SPECT) studies for the detection of decreases in the myocardial blood supply. Through the utilization of multiple postprocessing techniques, a single DECT acquisition may potentially detect obstructive coronary artery disease (CAD) and simultaneously provide information concerning the hemodynamic consequences of the detected lesions on myocardial perfusion (Ruzsics et al. 2008, 2009; Wang et al. 2011). DECT examination can also be performed during adenosine stress, improving the diagnostic accuracy for the detection of myocardial ischemia; this also adds incremental value to a coronary computed tomography angiography (CCTA) in the detection of hemodynamically significant coronary stenoses (Ko et al. 2011, 2012a). In recent practice, dual-source DECT of the heart has emerged as an attractive imaging modality for the evaluation of myocardial perfusion, with or without adenosine administration. This chapter provides a protocol setup and

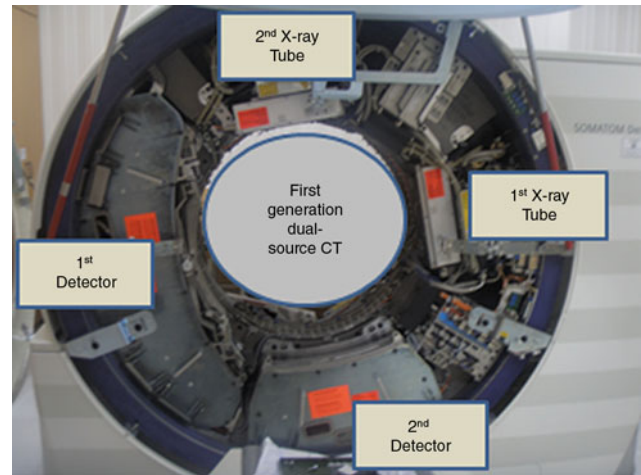


Fig. 1 Diagram of a dual-source DECT scanner. Dual-source CT with two X-ray tubes and two corresponding detector arrays mounted in the same gantry operates independently at different voltage settings (140 kV and 80/100 kV) and simultaneously acquires two data sets showing different attenuation levels

the characteristic features of dual-source DECT, and derives its benefits and limitations for DECT myocardial perfusion.

2 Principles of Material Decomposition in Dual-Energy CT

With dual-source CT in dual-energy mode, two X-ray tubes are operated independently at different voltages (80 or 100 kV and 140 kV), simultaneously acquiring two image datasets in the same anatomic location with two different X-ray spectra (Fig. 1). How does dual-source DECT obtain additional information regarding the elementary chemical composition of a scanned material? Material differentiation in CT is based on X-ray attenuation, as quantified in HUs. At low photon energies, X-ray attenuation is dominated by photoelectric absorption; at high photon energies, Compton scattering prevails. Low atomic number materials, such as fat and muscle, are affected by Compton scattering and show a small degree of reduction in the HU value when photon energy increases. On the contrary, higher atomic number materials, such as bone and iodine, are affected by the photoelectric absorption and show rapid decrease of HU value when photon energy increases (Fig. 2).

Iodine is a commonly used CT contrast agent; clinical observation has shown that iodine contrast agents have stronger enhancement at lower tube voltage settings. In dual-source DECT, we observe a greater photoelectric absorption by iodine at 80 kV than at 140 kV. This phenomenon occurs because the mean photon energy of the 80 kV beam (53 keV) is closer to the K-edge of iodine

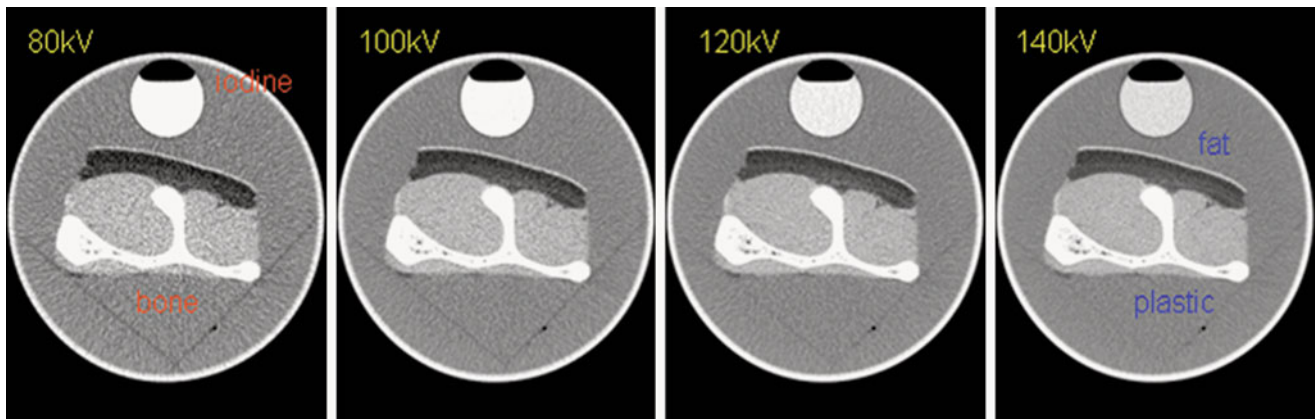


Fig. 2 Basic concept of DECT for material differentiation. Iodine has its maximum attenuation at 80 kV but its CT attenuation markedly decreases with increased voltage. The CT attenuation of bone changes much less when it is scanned with low kV as compared to high kV

(33 keV) than that of the 140 kV beam (71 keV). Accordingly, iodine-containing structures are more attenuating at 80 kV than at 140 kV. Dual-source DECT can allow material differentiation on the basis of such energy-dependent attenuation characteristics (Johnson et al. 2007).

Material-specific imaging in dual-source DECT is based on a mathematical algorithm termed “3-material decomposition.” This method is capable of measuring the relative concentrations of three pure constituent materials in scanned tissue by evaluating the attenuation properties of each voxel and by comparing these values with the attenuation coefficients of the three pure constituent materials at low and high kV. In the heart, the 3 materials usually analyzed are soft tissue, fat, and iodine. In addition, an iodine distribution image, or iodine distribution map, is produced via material decomposition along with virtual non-contrast images in which the iodine content has been subtracted from the contrast-enhanced images (Johnson et al. 2007; Vlahos et al. 2010).

3 Configuration of Dual-Source Dual-Energy CT

3.1 First Generation Dual-Source Dual-Energy CT (Siemens Definition)

Dual source CT is equipped with two orthogonally mounted X-ray tubes and two corresponding detector systems. The field of view of the B tube array is smaller (26 cm in diameter), compared with the A tube (50 cm in diameter), due to space limitations on the gantry of the dual-source CT scanner (Fig. 3a). Each detector comprises 40 detector rows, the 32 central rows having a 0.6-mm collimation slice width and the 4 outer rows on either side having a 1.2-mm

examination. The CT attenuation of fat increases as the kV setting is increased. Accordingly, changing the X-ray tube’s kV setting results in a material-specific change of attenuation (Reproduced with kind permission from Siemens Healthcare)

collimated slice width. Using the z-flying focal spot technique, each detector acquires 64 overlapping 0.6-mm slices per rotation. The shortest gantry rotation time is 330 ms. There is an 8 ms interval between the image acquisitions of the 2 tubes in the same plane. The two X-ray tubes are operated independently with respect to their voltage and current settings, allowing simultaneous acquisition of high and low X-ray energy spectra within a single scan, e.g., one tube (B tube) is operated at 100 kV while the other (A tube) is operated at 140 kV. The tube current can be adjusted separately for each kV level (e.g., 100 mAs/rotation at 140 kV and 165 mAs/rotation at 100 kV), permitting noise level matching the two datasets (Flohr et al. 2006; Peter-silka et al. 2008; Kang et al. 2010).

3.2 Second Generation Dual-Source Dual-Energy CT (Siemens Definition Flash)

The latest dual-source CT has several major technical improvements, including faster gantry rotation of 280 ms, increasing the scan field of the detector (increased detector z-coverage), increasing the field of view for detector B from 26 to 33 cm, high-pitch modes for rapid helical acquisition, and pre-patient filtration (Fig. 3b). Of these, pre-patient filtration is arguably the most important. This technical advance improves the discrimination of materials by minimizing the overlap of the two energy spectra. With pre-patient filtration, the lower-energy photons in the 140 kV beam are removed by a tin filter placed at the X-ray tube (Sn140 kV), resulting in a higher mean beam energy. This filtration increases the energy separation by minimizing the overlap of high and low kV spectra and, therefore, improves both the material differentiation and decomposition. In addition, radiation dose is reduced as the low-energy

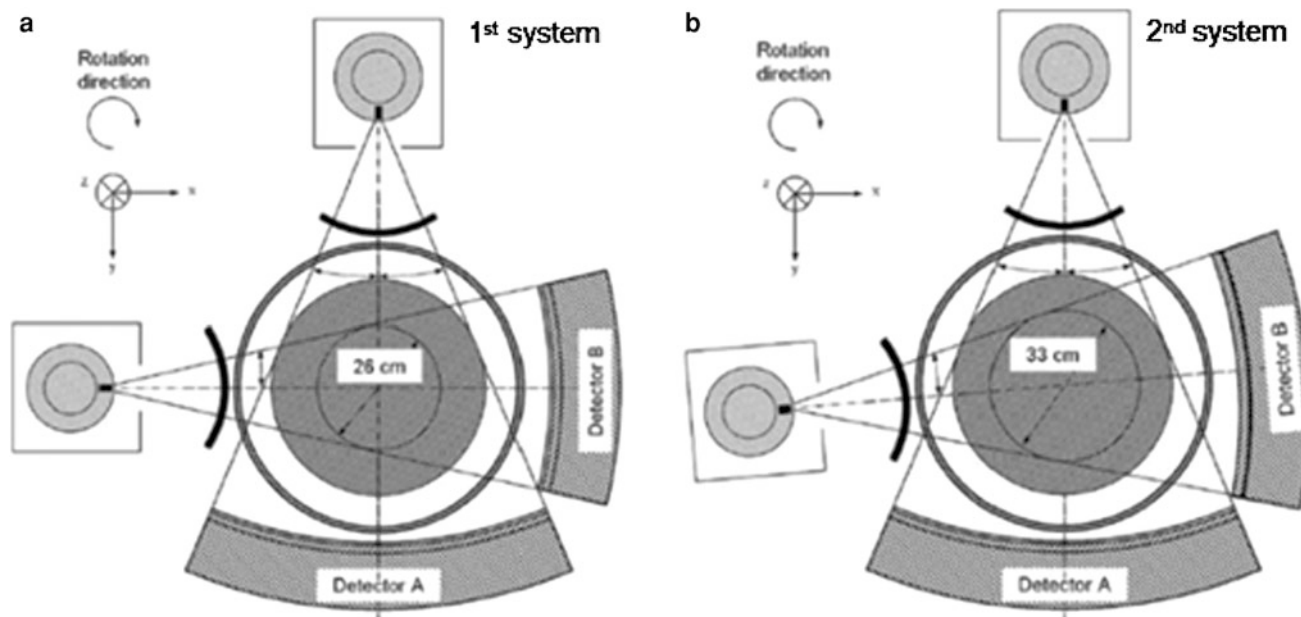


Fig. 3 Schematic illustration of first (Siemens SOMATOM Definition) and second (Siemens SOMATOM Definition Flash)- generation dual-source DECT systems. The first-generation dual-source CT system (a) has the A tube, which is associated with a 50 cm field of view for detector A and is operated at 140 kV, and the B tube, which

is associated with a 26 cm field of view for detector B and is operated at 80/100 kV. The second-generation dual-source CT system (b) has a larger 33 cm field of view for detector B, achieved by increasing the angle between the X-ray tubes and detectors from 90° to 94° (Reproduced with kind permission from Siemens Healthcare)

photons are removed from the high-energy X-ray tube spectrum. Pre-patient filtration facilitates the use of a 100 kV low-energy beam, which enables greater tissue penetration and less image noise, compared with 80 kV (Kang et al. 2010).

4 Methodology for Dual-Energy CT Image Acquisition

4.1 Image Acquisition of Rest Dual-Energy CT

DECT acquisition can be performed using the following parameters: 330-ms gantry rotation time, heart rate adaptive pitch of 0.2–0.43, $32 \times 2 \times 0.6$ -mm collimation with z-flying focal spot technique, and 165-ms temporal resolution. One tube of the dual-source CT system is operated with 82–114 mAs/rotation at 140 kV, the second tube with 165 mAs/rotation at 80 kV for slim (≤ 140 lbs) individuals, and 165 mAs/rotation at 100 kV for average-sized (≤ 200 lbs) and larger patients (Ruzsics et al. 2008). With the scout image, the anatomic range extends from 2 cm below the level of the tracheal bifurcation to the diaphragm in a craniocaudal direction. Oral β -blocker administration is given if the resting heart rate is higher than 70 beats per minute. The retrospectively gated scan uses electrocardiography (ECG)-based tube current modulation with the

Mindose protocol. Wider full-dose pulsing window (i.e., 35–75 %) is applied for faster and irregular heart rates, and narrow full dose windows (i.e., 60–80 %) for slower and more regular heart rates. Tube current reduction to 4 % was applied outside the adjusted pulsing windows.

DECT examinations are contrast enhanced, using the routine clinical contrast agent injection protocol, which is controlled by either the test-bolus or bolus-tracking technique. With the test-bolus technique, the time delay between the start of contrast injection and the start of data acquisition is determined by an injection of 20 ml of a non-ionic contrast agent at 6 ml/s through an 18-gauge intravenous antecubital catheter, followed by 30 ml of saline, using a dual-head power injector. The peak time of the test bolus enhancement, as measured by a repetitive scanning at the level of the aortic root, is used as the delay time. Actual contrast agent enhancement is achieved by injecting an initial bolus of undiluted contrast agent, which is then followed by a constant 50 ml volume of a 70 %/30 % saline/contrast agent mixture, and finally 30 ml of pure saline, all injected at 6 ml/s. The initial iodine bolus volume is computed per CT examination using the following formula: volume (milliliters) = duration of CT data acquisition (seconds) \times 6. If the duration of CT data acquisition is less than 10 s, a minimum of 60 ml of contrast medium is required (Ruzsics et al. 2008). There is no established optimal scan protocol (amount and speed of contrast

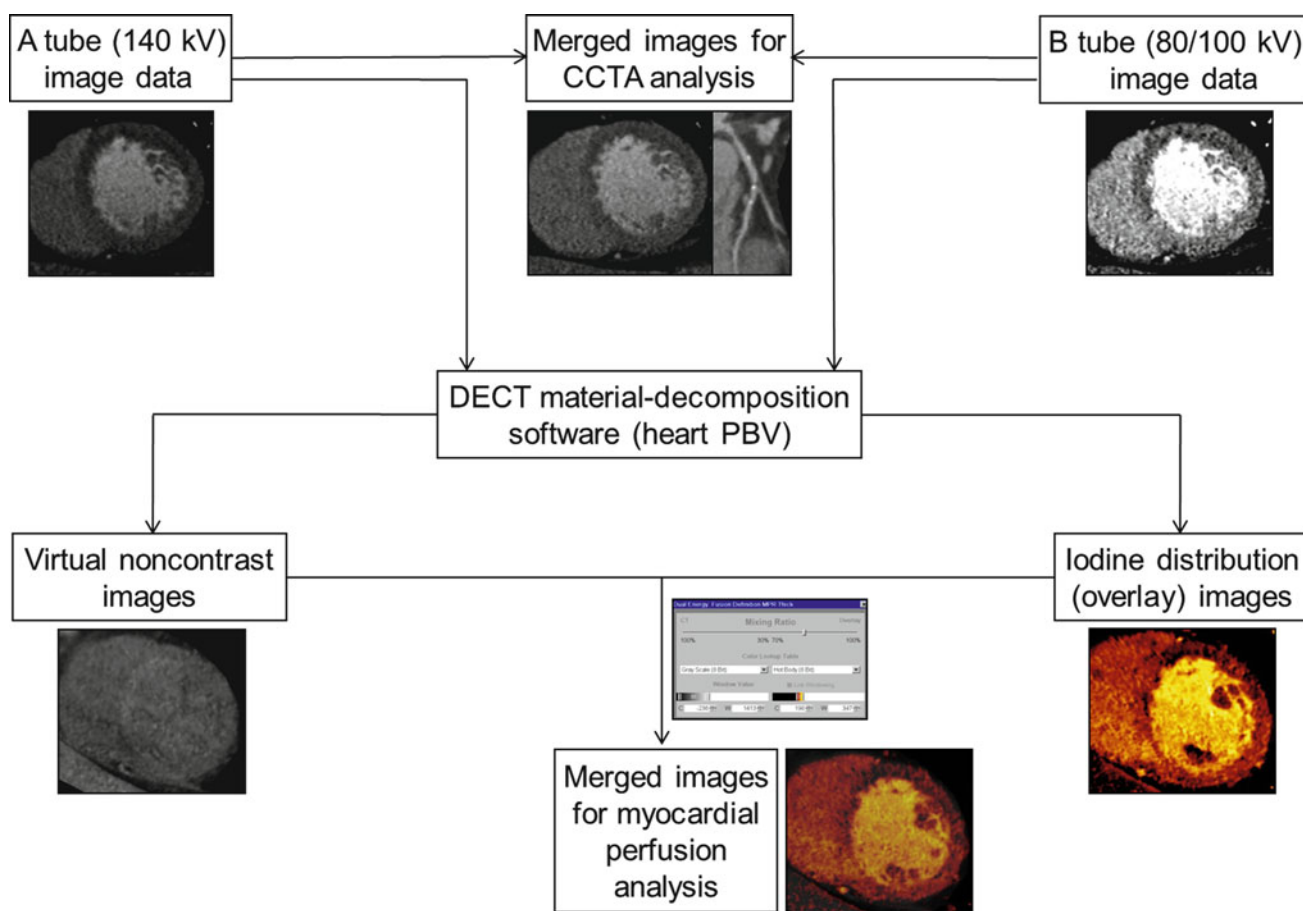


Fig. 4 Diagram of image postprocessing of DECT for analysis of myocardial perfusion. Merged images, which are produced by mixing 140 kV and 80/100 kV datasets at a ratio of 7:3, respectively, are equivalent to coronary CT angiography images obtained at approximately 120 kV. Using dual-energy material decomposition software, the iodine component is separated from the images obtained from high

(A tube) and low (B tube)-energy X-ray spectra and is displayed in color-coded iodine distribution (overlay) images. Grayscale virtual non-contrast images are generated by removing iodine from the source images. Final images are obtained by mixing iodine distribution images and virtual non-contrast images, typically at a ratio 7:3, for assessment of the myocardial blood pool

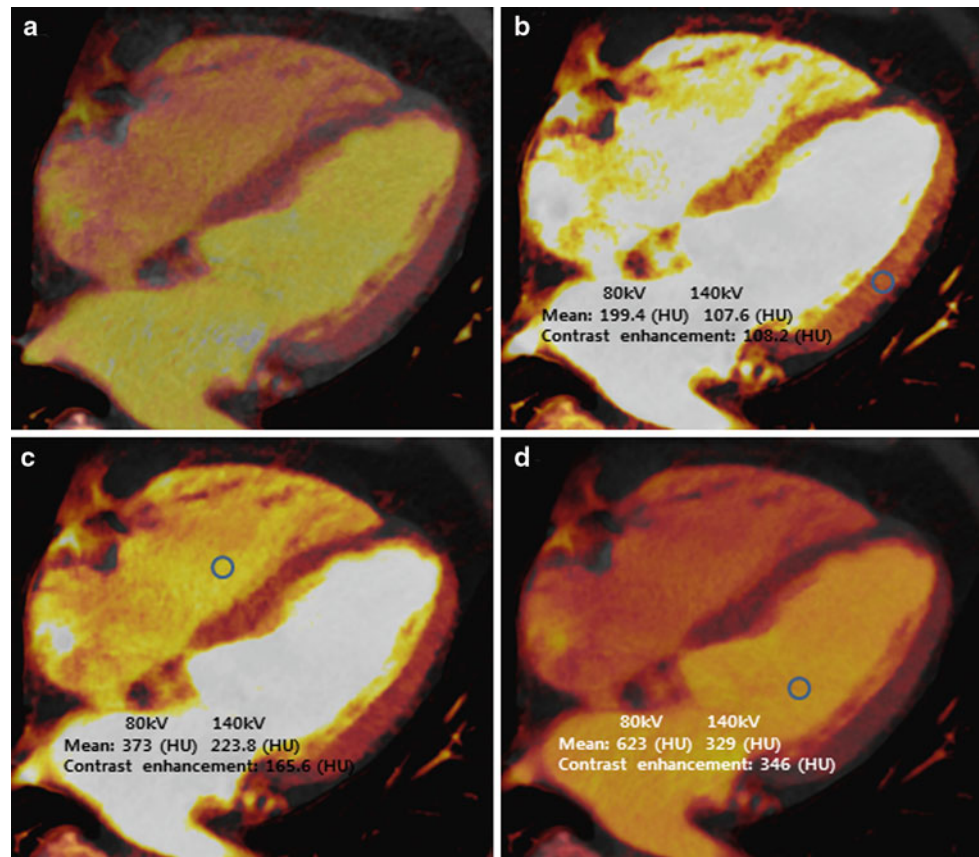
administration, scan delay time, etc.) with a bolus-tracking technique. In our center, with the bolus tracking technique, the region of interest is placed into the aortic root, and image acquisition is started seven seconds after the signal density level reaches the predefined threshold of 120 HU. For DECT examinations, a dual-head power injector is used to administer a 3-phase bolus at a rate of 4.5 ml/s. According to scan time and patient's body mass index, 60–80 ml of undiluted contrast agent is injected, followed by 45 ml of 70 %/30 % contrast agent/saline mixture, and finally 45 ml of saline (Ko et al. 2011).

4.2 Image Acquisition of Stress Dual-Energy CT

Patients undergoing stress DECT perfusion are instructed not to drink coffee or tea, and not to have oral β -blockers for at least 24 h prior to the examination. Two intravenous lines

are inserted (18-gauge for contrast medium delivery; 20-gauge for adenosine infusion). Before the examination, the heart rate of each patient is measured. Beta-blockers and nitroglycerine are avoided because of their impact on myocardial perfusion. Stress DECT perfusion is performed using the same imaging parameters as the rest DECT. Blood pressure, standard ECG, and clinical symptoms are carefully monitored during the adenosine infusion and after imaging. Any adverse side effect (e.g., severe tachycardia, tachyarrhythmia, allergic reaction) is grounds for termination of the examination. Adenosine infusion is started at a constant rate of 140 $\mu\text{g}/\text{kg}/\text{min}$ over six minutes. Retrospectively gated imaging with ECG-based tube current modulation (Mindose protocol) and pitch adaptation is obtained four minutes after the initiation of the adenosine infusion. In our center, contrast agent administration with the bolus tracking technique is the same as that in rest DECT, except that image acquisition starts nine seconds after the signal density level reaches the predefined

Fig. 5 Normalization of iodine distribution map. **a** Color-coded “iodine distribution map,” which is superimposed on grayscale “virtual non-contrast image” multiplanar reformat of the myocardium. Because of a broad range of iodine concentration within the myocardium, the map must be normalized to an area of normal myocardial perfusion **b**, the right ventricle **c**, or the left ventricle **d**. Usually, areas of highest iodine content in the myocardium are recommended for normalization of the iodine distribution map



threshold of 120 HU at the aortic root for increasing differences in contrast enhancement between ischemic and non-ischemic myocardium (Ko et al. 2011).

4.3 Image Reconstruction of Dual-Energy CT

The data sets for the assessment of coronary artery and myocardial perfusion are reconstructed during the phase that depicts the fewest motion artifacts within the full-dose window, usually in the mid-diastolic phase, with reconstruction windows set at 60–75 % of the R–R interval. The recently implemented automatic phase finding algorithm (BestPhaseTM) is useful for identifying optimal reconstruction phases during systole and diastole without user interaction.

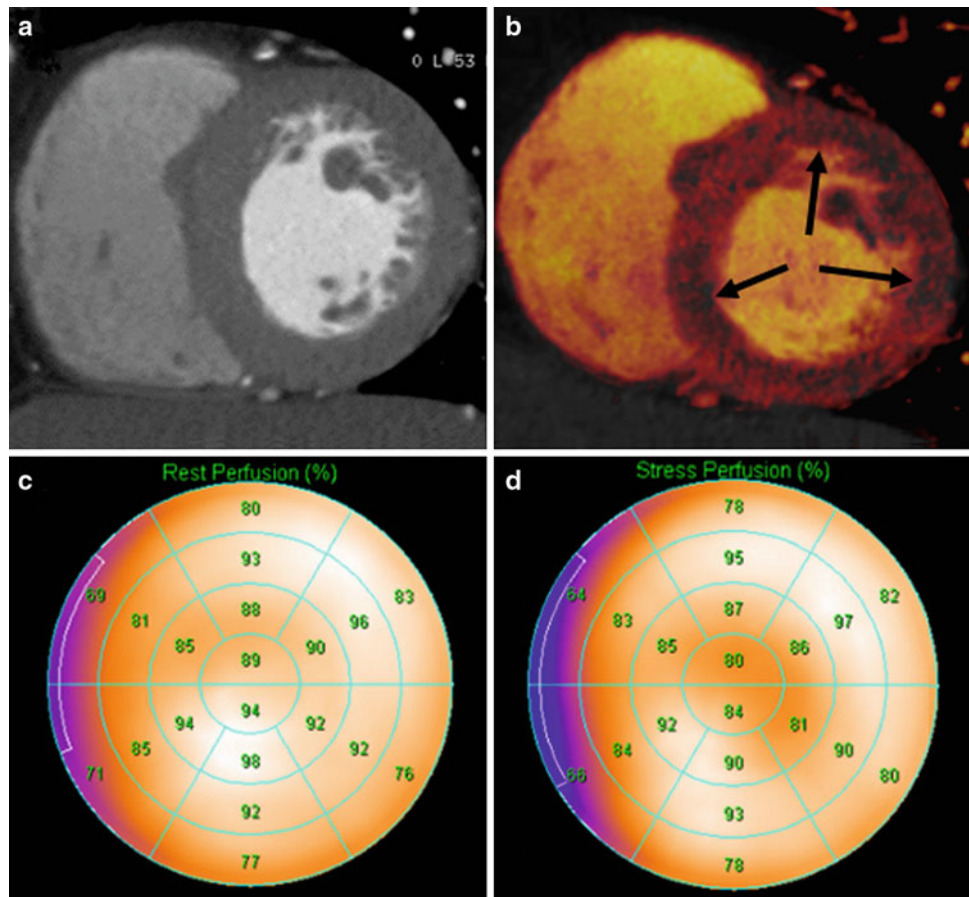
Standard DECT cardiac scan protocol includes a series of different image reconstructions from the same contrast enhanced DECT scan. The first set of transverse gray-scale images is reconstructed using a B26f kernel with a temporal resolution of 165 ms, slice thickness of 0.75 mm, and slice increment of 0.4 mm, for each tube-detector array. By merging 70 % of the high (140 kV) X-ray spectrum and 30 % of the low (80/100 kV) X-ray spectrum, a series of grayscale images is created that is similar to an image

obtained using a single-energy CT at 120 kV. This series aims at optimizing the spatial and contrast resolution, and is used for clinical cardiac CT interpretation of coronary artery morphology and stenoses. For the analysis of myocardial perfusion, high-voltage and low-voltage data are reconstructed separately using a dedicated dual-energy convolution kernel (D26f or D30f) with a temporal resolution of 330 ms, slice thickness of 0.75 mm, and an increment of 0.4 mm (Ruzsics et al. 2008; Ko et al. 2011; Schwarz et al. 2008). Ruzsics et al. used a 1.5-mm slice thickness and a 0.5-mm increment to optimize the signal/noise ratio (Schwarz et al. 2008).

4.4 Post-Processing, Display, and Analysis

A single DECT data acquisition can be used to generate a virtual non-contrast image, two single-energy images based on high (140 kV) and low (80 or 100 kV) X-ray spectra, a dual-spectrum merged image, and an iodine distribution image; the iodine distribution can also be superimposed in color over the merged image (merged image with color-coded iodine distribution) (Fig. 4). The reconstructed high- and low-voltage data sets, obtained with DECT, are loaded into a dedicated algorithm, heart perfusion blood volume

Fig. 6 Comparison of stress DECT perfusion and myocardial perfusion SPECT for balanced ischemia. The CT perfusion image at rest (**a**) does not show any perfusion defects in the left ventricular (LV) myocardium. DECT-based iodine distribution mapping during adenosine infusion (**b**) reveals concentric blood pool deficits (*arrows*) in mid LV myocardium. Findings are not correlated with myocardial perfusion SPECT acquired at rest (**c**) and stress (**d**), which reveal limitation of myocardial perfusion SPECT for balanced ischemia. Conventional coronary angiogram (not shown) reveals significant stenoses at the left main coronary artery and the 3 major epicardial coronary arteries



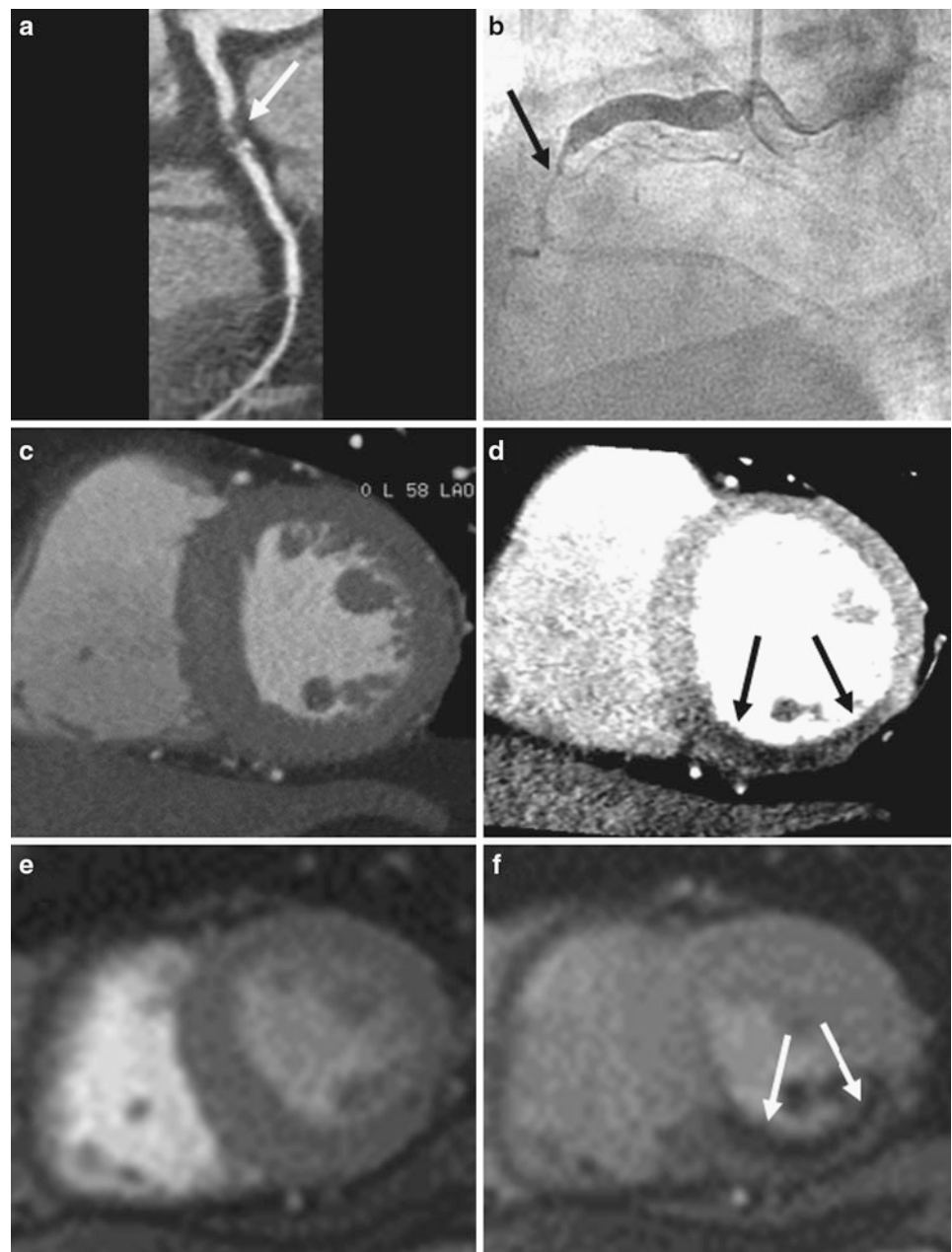
(heart PBV), for the evaluation of myocardial perfusion. The heart PBV algorithm is incorporated in the dual-energy-image post-processing software application of the Syngo-Multimodality Workplace (syngo Dual Energy, Siemens). Differences in the attenuation of iodine at the two different energies allow for the computation of the iodine distribution within the myocardium and the generation of virtual non-contrast images. The attenuation of epicardial fat on the merged reconstruction is measured for fat calibration of the heart PBV algorithm. In addition, the broad range of iodine concentrations that this study produces requires normalization of the iodine distribution map to the areas of normal myocardial perfusion (Schwarz et al. 2008). Areas with high iodine content, including the myocardium or any cardiac chamber, can be chosen for this process; we primarily normalize using the right ventricular lumen (Fig. 5). The color-coded iodine distribution maps are superimposed onto a grayscale multiplanar reformats of the myocardium. We employ a 70 % overlay of the iodine distribution map over the merged reconstruction with 5-mm thick multiplanar-reformatted short and long axis views for the evaluation of myocardial perfusion. Myocardial blood pool deficits on DECT-based iodine distribution maps are defined as contiguous, circumscribed areas of decreased or

absent iodine content within the left ventricular (LV) myocardium, relative to the remote normal myocardium. Myocardial blood pool deficits are assessed quickly and accurately by visual analysis because DECT-based iodine distribution map highlights the areas of decreased iodine in the LV myocardium. Accordingly, visual analysis is mainly used over quantitative analysis for the detection of myocardial blood pool deficits. The AHA/ACC-segmental model (17 segment model) is used to report the findings at perfusion analysis (Schwarz et al. 2008).

5 Overview of Imaging Modalities for Coronary Artery Disease

Conventional coronary angiography (CCA) is considered as the established, anatomic gold standard for the diagnosis of CAD by direct visualization and grading of coronary stenosis. However, CCA is invasive, costly, and not without risk. In addition, anatomical assessment of the hemodynamic significance of coronary stenosis, determined by CCA, correlates poorly with functional assessment of the fractional flow reserve (FFR) (Chandrasekar et al. 2001; Meijboom et al. 2008). SPECT myocardial perfusion

Fig. 7 Representative example of single-energy CT perfusion identifying single-vessel disease. Curved multiplanar reformatted coronary CT angiographic image (a) shows total occlusion with non-calcified plaque (arrow) in the middle segment of the right coronary artery (RCA). Conventional coronary angiogram (b) confirms the subtotal occlusion (arrows) in the middle RCA. Rest (c) and stress (d) single-energy CT perfusion images reveal reversible transmural perfusion defects (arrows) in the mid inferoseptal and the inferior left ventricular myocardium. Findings are in good correlation with cardiac MR acquired at rest (e) and stress (f), which reveal reversible subendocardial perfusion defect (arrows) in the same myocardial areas



imaging (MPI) is an accepted clinical standard for the detection and quantification of myocardial ischemia. However, SPECT has the disadvantages of poor spatial resolution, radiation exposure, and attenuation artifacts. In addition, SPECT does not detect subclinical, non-obstructive coronary atherosclerosis and consistently underestimates the true extent of multivessel CAD (balanced ischemia) (Hachamovitch et al. 1996; Heller et al. 2009) (Fig. 6). Recent technical advances and improvements in cardiac CT have allowed for the non-invasive detection of significant coronary stenosis with high diagnostic accuracy. In addition, CCTA visualizes the coronary vessel wall, thereby, providing plaque composition and size, and

vascular remodeling (Mühlenbruch et al. 2007; Vanhorenacker et al. 2007). However, CCTA has a tendency to overestimate the severity of CAD in patients with high pretest probability of CAD. Furthermore, in its current form, CCTA does not provide information regarding the hemodynamic significance of coronary stenosis. Determining the hemodynamic significance of a morphologically intermediate stenosis (50–70 % lumen reduction) remains crucial before a referral for the revascularization treatment (Meijboom et al. 2008; Gaemperli et al. 2008). Consequently, there is great interest in combining non-invasive CCTA with SPECT-MPI. However, the hybrid imaging system requires the cost associated with combining two

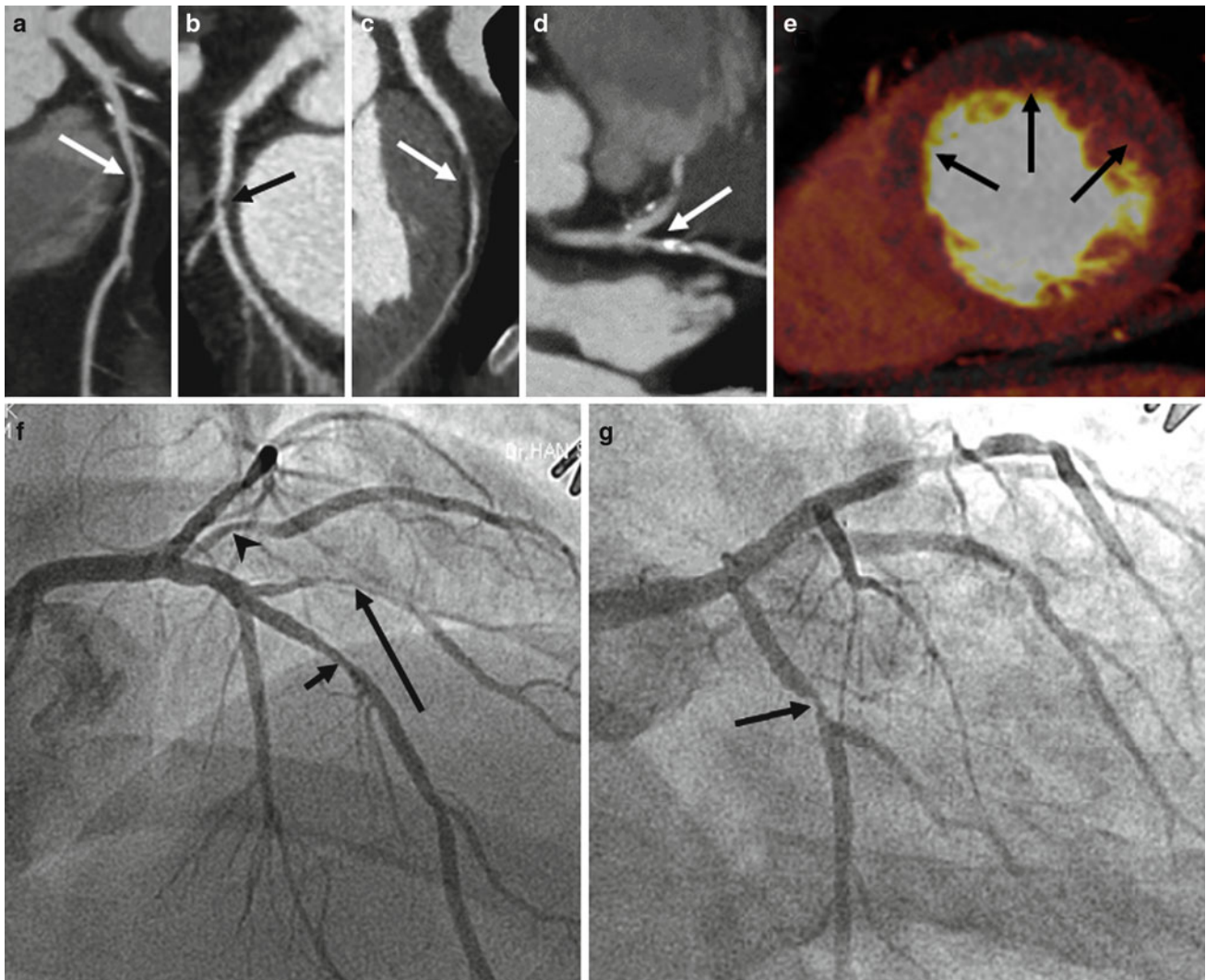


Fig. 8 Representative example of rest DECT perfusion identifying multivessel disease. Coronary CT angiograms (a–d) show significant stenoses with mixed calcified and non-calcified plaques (a, arrow) in the middle segment of the left anterior descending coronary artery (LAD), non-calcified plaque (b, arrow) in the proximal segment of the left circumflex artery (LCx) and the first diagonal branch (D1, arrow in

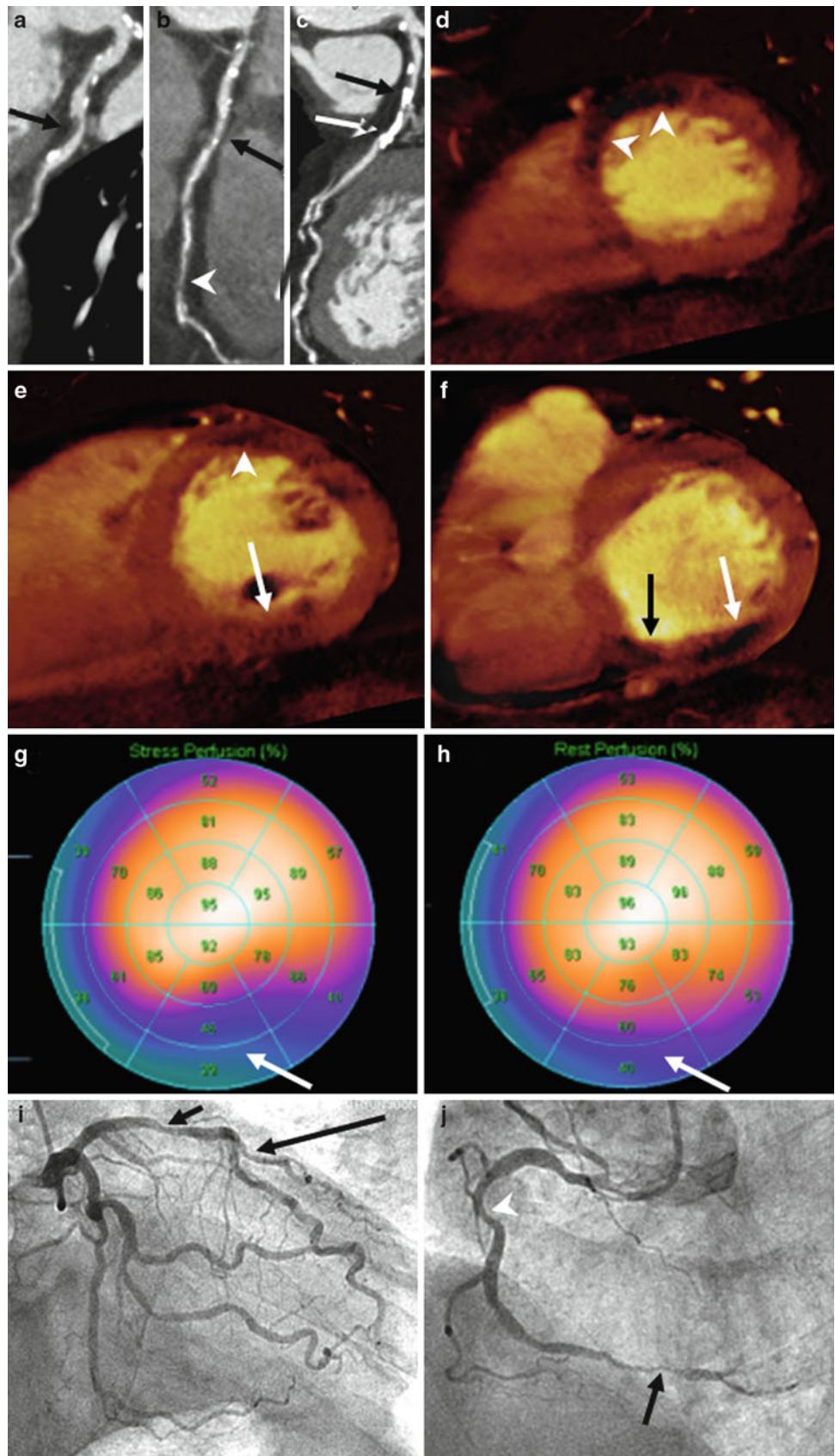
c) and calcified plaque (d, arrow) in the ramus intermedius (RI). DECT-based iodine distribution mapping at rest (e) reveals blood pool deficits (arrows) in the mid anteroseptum, anterior and anterolateral left ventricular myocardium. Conventional coronary angiograms (f, g) confirm the presence of significant stenoses in LAD (short arrow), D1 (long arrow), RI (arrowhead), and LCx (middle arrow)

imaging modalities and increases the radiation burden to the patient (Santana et al. 2009; Gaemperli et al. 2007). Recently, cardiac magnetic resonance (MR) with adenosine stress has been established as a non-invasive diagnostic modality with a high diagnostic accuracy for inducible perfusion defect, without radiation exposure or attenuation artifacts. In particular, cardiac MR has superior spatial resolution over SPECT, and thereby allows for a depiction of subendocardial perfusion defects in patients with microvascular disease. However, adenosine stress cardiac MR perfusion can be limited by availability, claustrophobia, obesity, poor gating, motion artifacts, and contraindications, such as pacemaker or defibrillators (Nandalur et al. 2007; Watkins et al. 2009).

6 Overview of Single-Energy CT Perfusion Imaging

Myocardial perfusion is strictly defined as the flow of blood to the myocardium and is often used as a relative myocardial blood volume or regional level of myocardial iodine enhancement. CT myocardial perfusion images are obtained using a static (single-phase first-pass myocardial enhancement imaging) or dynamic acquisition (quantitative time resolved myocardial perfusion imaging). Several CT-based MPI studies in animal models have demonstrated that the concentration of iodinated contrast agent in myocardium is directly proportional to the measured CT attenuation

Fig. 9 Comparison of coronary CT angiography, rest DECT perfusion, myocardial perfusion SPECT, and conventional coronary angiography. Coronary CT angiograms (a–c) show significant stenoses with non-calcified plaque (*arrow*) in the proximal segment of the left circumflex artery (a) and mixed calcified and non-calcified plaques (*arrow*) in the middle segment of the right coronary artery (RCA) and subtotal occlusion with non-calcified plaque (*arrowhead*) in the distal segment of RCA (b). Severe calcification (*arrows*) can render the proximal left anterior descending coronary artery (LAD) uninterpretable regarding the presence of significant stenosis (c). DECT-based iodine distribution mapping at rest (d–f) reveals blood pool deficits in the apical to mid anterior and apical septum (*arrowheads*) and mid to basal inferior (*arrows*) left ventricular (LV) myocardium. Myocardial perfusion SPECT at stress (g) and rest (h) show partially reversible perfusion defects (*arrows*) in inferior and inferolateral LV myocardium, corresponding to old myocardial infarction in RCA territory. However, SPECT images do not detect ischemic perfusion defects in LAD territory which is shown on rest DECT perfusion images. Conventional coronary angiograms (i, j) confirm the presence of significant stenoses in the proximal LAD (i, *short arrow*), D1 (i, *long arrow*), middle RCA (j, *arrowhead*), and distal RCA (j, *middle arrow*)



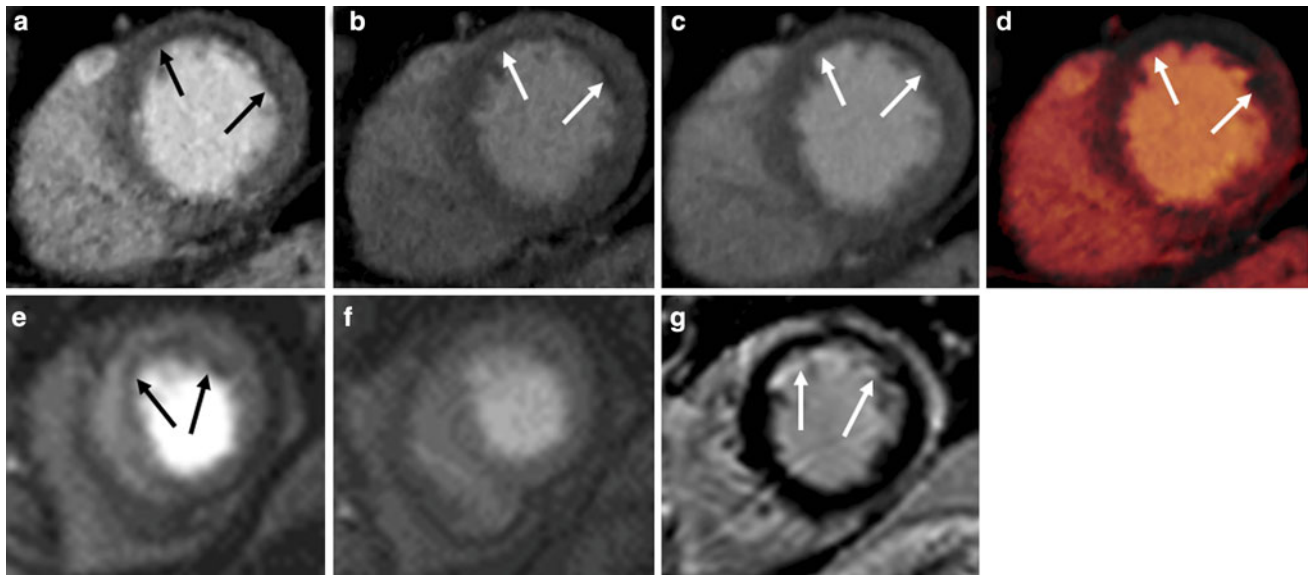


Fig. 10 Rest DECT-based iodine distribution map compared with single-energy CT spectra. Better visualizes blood pool deficits (*arrows*) in the apical anterior and lateral left ventricular (LV) myocardium compared to reconstruction images using 80-kV CT spectra (a), 140-kV CT spectra (b), and merged data (c). DECT-based

iodine distribution map at rest (d). Stress (e) and rest (f) perfusion and delayed contrast-enhanced (g) cardiac MR images confirm subendocardial myocardial infarction with peri-infarct ischemia (*arrows*) in the apical anterior and lateral LV wall

number; that iodinated contrast agent has similar pharmacokinetics to gadolinium-based contrast agents used for stress cardiac MR perfusion; that adenosine stress CT perfusion imaging correlates well with microsphere-derived myocardial blood flow; and, that ischemic myocardial perfusion defect can be diagnosed by an adenosine-induced stress CT perfusion imaging (George et al. 2006, 2007). Studies using adenosine-induced stress CT perfusion imaging have shown good diagnostic accuracy for the detection of ischemic myocardium caused by hemodynamically significant coronary artery stenosis, and increasing the value of CCTA through the detection of hemodynamically significant CAD (Blankstein et al. 2009; Rocha-Filho et al. 2010; Ko et al. 2012b) (Fig. 7). More recently, dynamic CT perfusion has provided results comparable to cardiac MR perfusion for the differentiation between normal and ischemic myocardium. Dynamic CT perfusion has also provided an incremental diagnostic value for the detection of hemodynamically significant coronary stenosis by quantifying myocardial blood flow (Bamberg et al. 2011). With the technical advances of multidetector computed tomography (MDCT), including dual-source CT and wide-area detector CT, CT has grown increasingly capable. By combining direct visualization and grading of coronary stenosis and plaque visualization obtained by CCTA with myocardial perfusion imaging provided by CT perfusion, CT is a single technological modality advantageously poised to provide a potential one-stop shop for the coronary risk assessment and possibly the approach to coronary intervention.

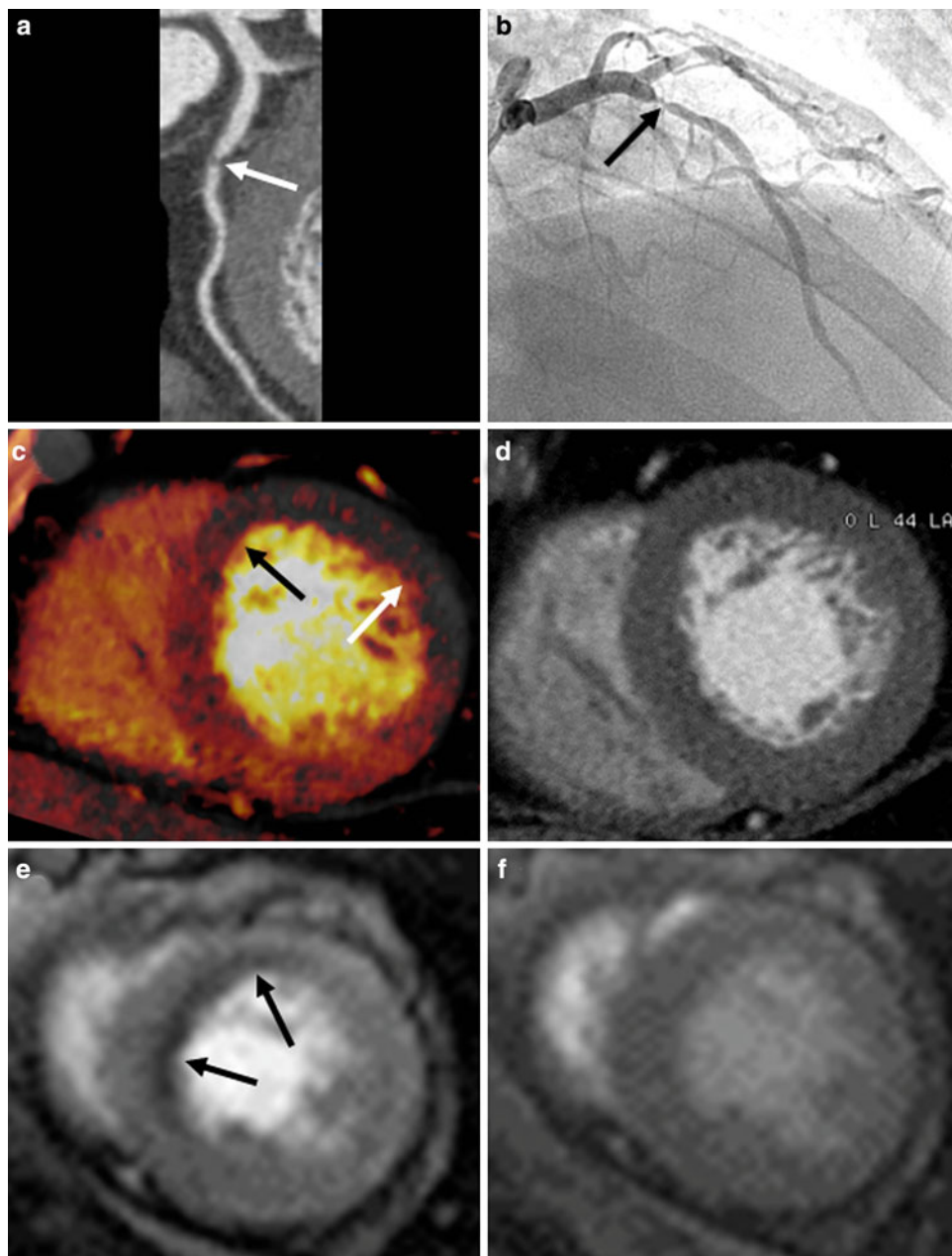
7 Dual-Energy CT Perfusion Imaging

7.1 Dual-Energy CT at Rest for Myocardial Perfusion

Rest DECT perfusion is acquired using retrospective ECG-gating with tube current modulation and a single-phase first-pass contrast enhancement protocol. With two synchronous CT acquisitions at different tube voltages, DECT allows for the assessment of myocardial perfusion status (or myocardial blood volume) by analyzing the iodine distribution within the myocardium (Fig. 8). The clinical evidence supporting the accuracy and feasibility of rest DECT for the assessment of myocardial perfusion deficits comes from three published single-center studies. Ruzsics et al. (2008) performed the first systematic investigation into the usefulness of cardiac DECT for diagnosing CAD and myocardial ischemia; they demonstrated that DECT had 91 % sensitivity and 91 % specificity with 91 % accuracy, in comparison with SPECT, for detecting any type of myocardial ischemia on a segmental basis; compared to CCA, DECT was found to have 92 % sensitivity, 79 % specificity, and 90 % accuracy for detecting the myocardial blood pool deficits on a segmental basis. In a recent study by Ruzsics et al. (2009), 36 patients with equivocal or incongruous SPECT results underwent single-phase, contrast-enhanced DECT at rest. DECT correctly identified 85 of 89 (96 %) fixed perfusion defects, and 60 of 68 (88 %) reversible myocardial perfusion defects. Overall,

Fig. 11 Representative example of stress DECT perfusion.

Curved multiplanar reformatted coronary CT angiographic image (a) shows severe stenosis with non-calcified plaque (arrow) in the proximal segment of the left anterior descending coronary artery (LAD). Conventional coronary angiogram (b) confirms the presence of severe stenosis (arrow) in the proximal LAD. DECT-based iodine map during adenosine infusion (c) reveals transmural blood pool deficits (arrows) in the apical septum, anterior and lateral left ventricular (LV) myocardium. The rest CT perfusion image (d) does not show any perfusion defects in the LV myocardium. Cardiac MR images acquired at stress (e) and rest (f) show reversible subendocardial perfusion defects (arrows) in the apical septal and anterior LV myocardium. The extent of stress-induced myocardial perfusion defect is larger on stress DECT than on stress cardiac MR



DECT had a sensitivity of 92 % and a specificity of 93 % with an accuracy of 93 % for type-independent detection of myocardial perfusion defects seen on SPECT. Interestingly, rest DECT is able to depict reversible perfusion defects only seen on stress SPECT images (Fig. 9). Although DECT iodine distribution maps at rest had a sensitivity of 88 %, a specificity of 89 %, and accuracy of 89 % for the detection of reversible perfusion defect, performance of rest DECT was substantially lower for the detection of reversible perfusion defects than that of mixed and fixed perfusion defects (Ruzsics et al. 2009). The physiological mechanism behind such a concordance remains controversial as DECT was not performed under stress. Possible explanations for DECT

detection of reversible perfusion defects, as hypothesized by Ruzsics et al. (2008, 2009), include the superior spatial resolution of CT for smaller areas of ischemia compared with SPECT, an intrinsic vasodilatory effect of the iodinated contrast agent, and different myocardial distribution kinetics of the iodinated contrast agent compared with the radiopharmaceutical tracers of SPECT.

Most recently, Wang et al. (2011) demonstrated on a per-vessel basis that sensitivity, specificity, and accuracy of DECT coronary angiography without DECT perfusion were 82, 91, and 86 %, respectively; with the addition of DECT perfusion, an overall improvement to 90, 86, and 88 %, respectively, was observed. This study demonstrated an

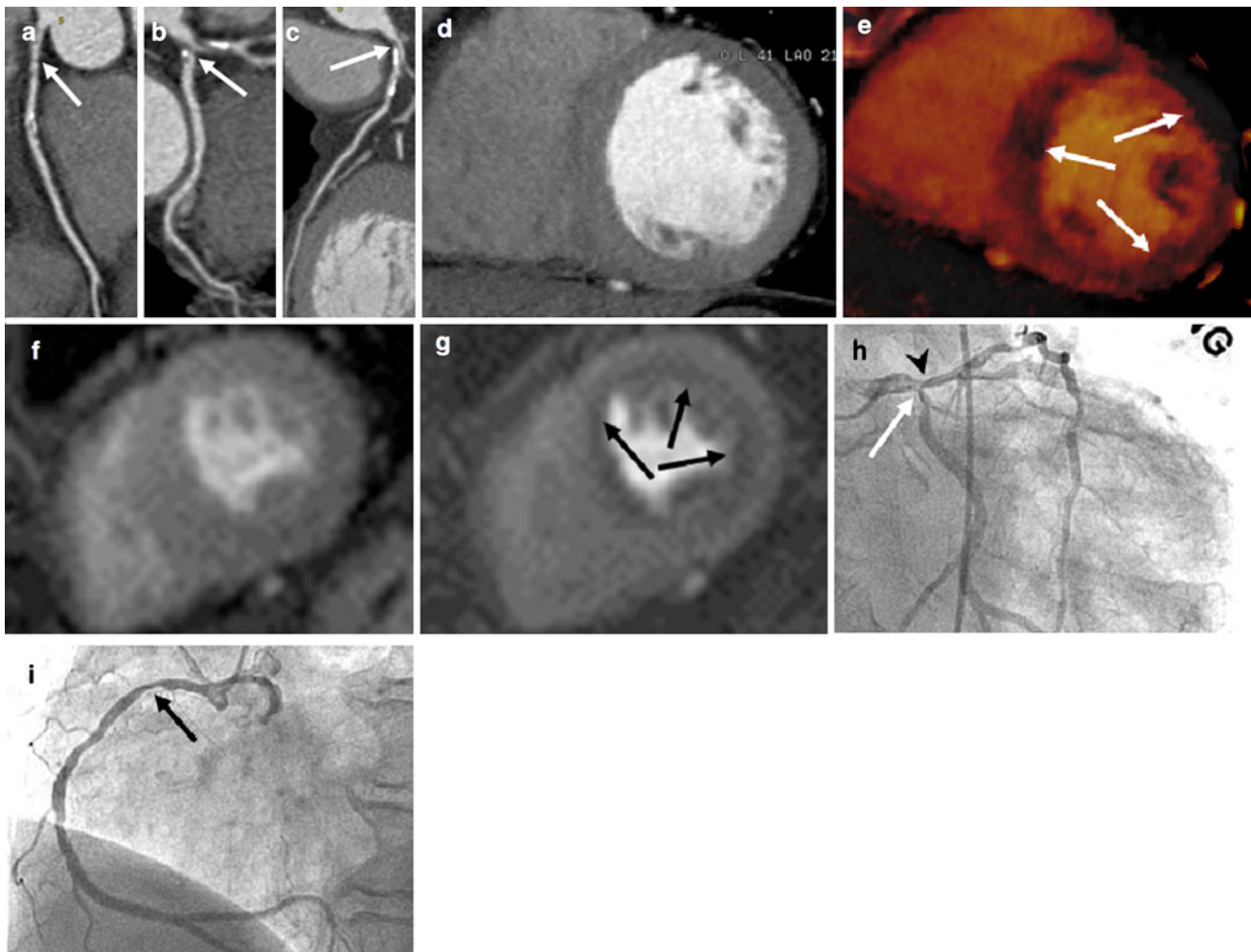


Fig. 12 Example of stress DECT perfusion for multivessel coronary artery disease. Curved multiplanar reformatted coronary CT angiographic images (**a–c**) show significant stenoses with non-calcified plaque (**a**, *arrow*) in the proximal segment of right coronary artery (RCA) and mixed calcified and non-calcified plaque (**b**, *arrow*) in the ostia of the left circumflex artery (LCX) and the left anterior coronary artery (LAD) (**c**, *arrow*). The CT perfusion image at rest (**d**) does not show any perfusion defects in the left ventricular (LV) myocardium.

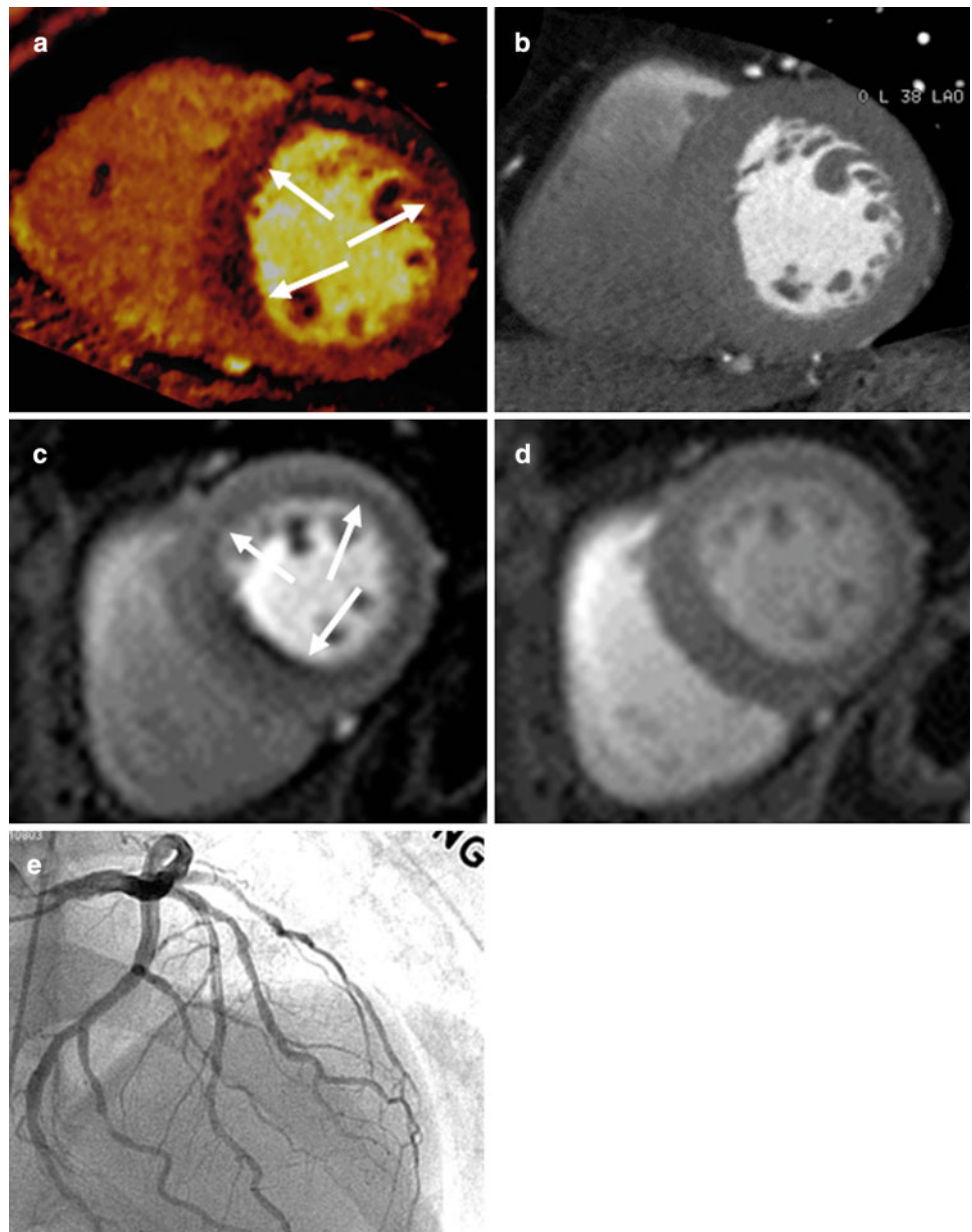
DECT-based iodine distribution map during adenosine infusion (**e**) reveals concentric blood pool deficits (*arrows*) in mid LV myocardium. Findings are in good correlation with cardiac MR acquired at rest (**f**) and stress (**g**), which reveal a reversible subendocardial perfusion defect (*arrows*) in the same myocardial areas. Conventional coronary angiogram findings (**h**, **i**) confirm the presence of significant stenoses in LAD ostium (**h**, *arrowhead*), LCx ostium (**h**, *arrow*), and proximal RCA (**i**, *arrow*)

incremental value of DECT on the detection of CAD (Fig. 9).

DECT-based color-coded iodine distribution map might be more sensitive to the detection of hypoperfused myocardium than single-energy CT-based gray scale image (Fig. 10). Arnoldi et al. (2011) compared the performance of cardiac CT on the basis of single-energy image reconstructions, merged image reconstructions, and DECT iodine distribution maps for the detection of reversible and fixed myocardial perfusion deficits seen on SPECT. They demonstrated that the four image reconstruction strategies had relatively similar, high specificity for the detection of perfusion deficits on SPECT. However, sensitivity, negative

predictive value, and accuracy for mixed perfusion deficits were highest with DECT iodine maps and were 91, 97, and 93 %, respectively. In addition, DECT iodine distribution maps had highest area under the curve values (0.84–0.93) for both observers in the detection of purely fixed and mixed perfusion defects seen on SPECT. These results might be explained by the distribution map of iodinated contrast material, based on DECT-based material decomposition, is better suited than visual analysis in the differences in CT attenuation values between ischemic and non-ischemic myocardium. DECT may be helpful to improve the specificity of myocardial single-phase first-pass enhancement CT imaging.

Fig. 13 Example of stress DECT perfusion for microvascular angina. DECT-based iodine distribution mapping during adenosine infusion (**a**) reveals subendocardial blood pool deficits (*arrows*) in the mid anterior, septal, and lateral left ventricular (LV) myocardium. The rest CT perfusion (**b**) does not show any perfusion defects in the LV myocardium. Cardiac MR images acquired at stress (**c**) and rest (**d**) reveal a reversible subendocardial perfusion defect (*arrows*) in the entire mid LV myocardium. Extent of stress-induced myocardial perfusion defect is larger on stress cardiac MR than on stress DECT. Conventional coronary angiogram finding (**e**) shows the left coronary dominance without any significant stenoses. These findings are consistent with microvascular angina



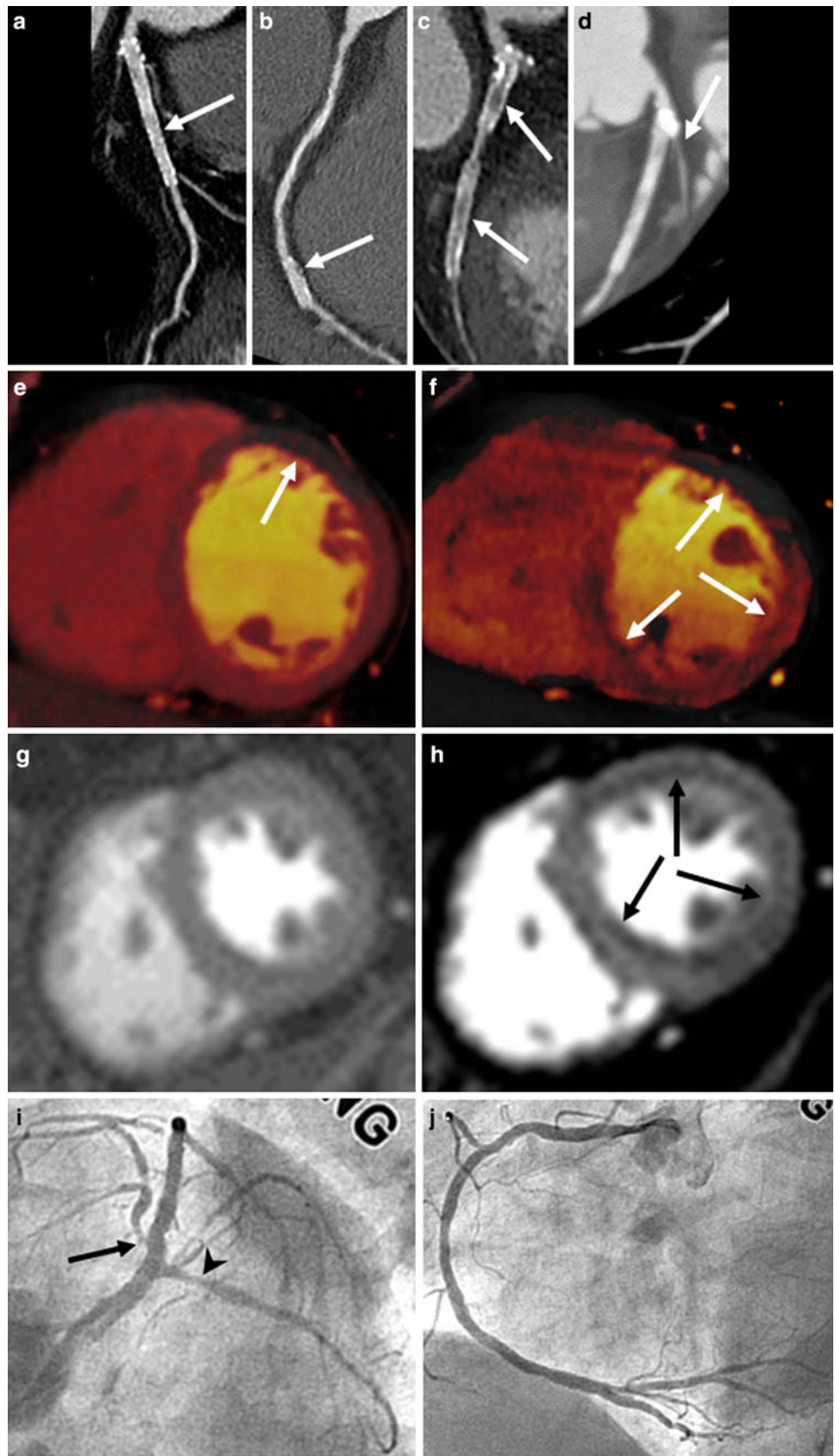
These studies can be summarized as follows: (1) DECT allows analysis of the iodine distribution within the myocardium by exploiting the absorption characteristics of iodine at different X-ray energies, (2) DECT allows the reproducible differentiation of iodine distribution within the myocardium to detect myocardial blood pool deficits in a good correlation with a clinical reference standard, such as SPECT, (3) DECT acquired at rest is able to detect areas of reversible, stress induced perfusion deficits as seen on SPECT, (4) DECT iodine distribution maps have good diagnostic performance for the detection of fixed and mixed myocardial blood pool deficits compared with single-energy CT spectra, and (5) rest DECT perfusion may improve the diagnostic performance of the detection of CAD

(synergistic clinical value). Accordingly, DECT imaging of the heart enable the integrative assessment of the coronary artery morphology and the myocardial blood supply in patients with known or suspected CAD.

7.2 Dual-Energy CT Under Stress for Myocardial Perfusion

Rest DECT perfusion had a much lower positive predictive value (26 %) for the detection of purely reversible perfusion defects than that of the mixed (85 %) and fixed (59 %) perfusion defects on per-myocardial segmental analysis (Arnoldi et al. 2011). The result suggests that DECT

Fig. 14 Example of rest and stress DECT perfusion for stent evaluation. Curved multiplanar reformatted coronary CT angiographic images (a–d) show a patent stent (arrow) in the big first diagonal branch (D1, a) and the distal segment of the right coronary artery (RCA, b) but significant in-stent restenosis (arrows) in the proximal and distal segments of the left circumflex artery (LCx, c). In addition, significant stenosis (arrow) is noted at the ostium of the first obtuse marginal branch (OM1, d). DECT-based iodine distribution map at rest (e) reveals blood pool deficits (arrows) in the mid anterior LV myocardium. Stress DECT-based iodine distribution map (f) shows blood pool deficits (arrows) in the mid anterior, inferoseptal, inferior, and lateral LV myocardium. Findings are in good correlation with cardiac MR acquired at rest (g) and stress (h), which reveal reversible subendocardial perfusion defect areas (arrows) in the same myocardial areas. Conventional coronary angiograms (i, j) show significant stenosis (arrow) in the ostium of the left anterior descending coronary artery (i) and also significant in-stent restenosis (arrowhead) in the proximal LCx stent (i). There are no in-stent restenosis in the big D1 stent (i) and distal RCA stent (j)



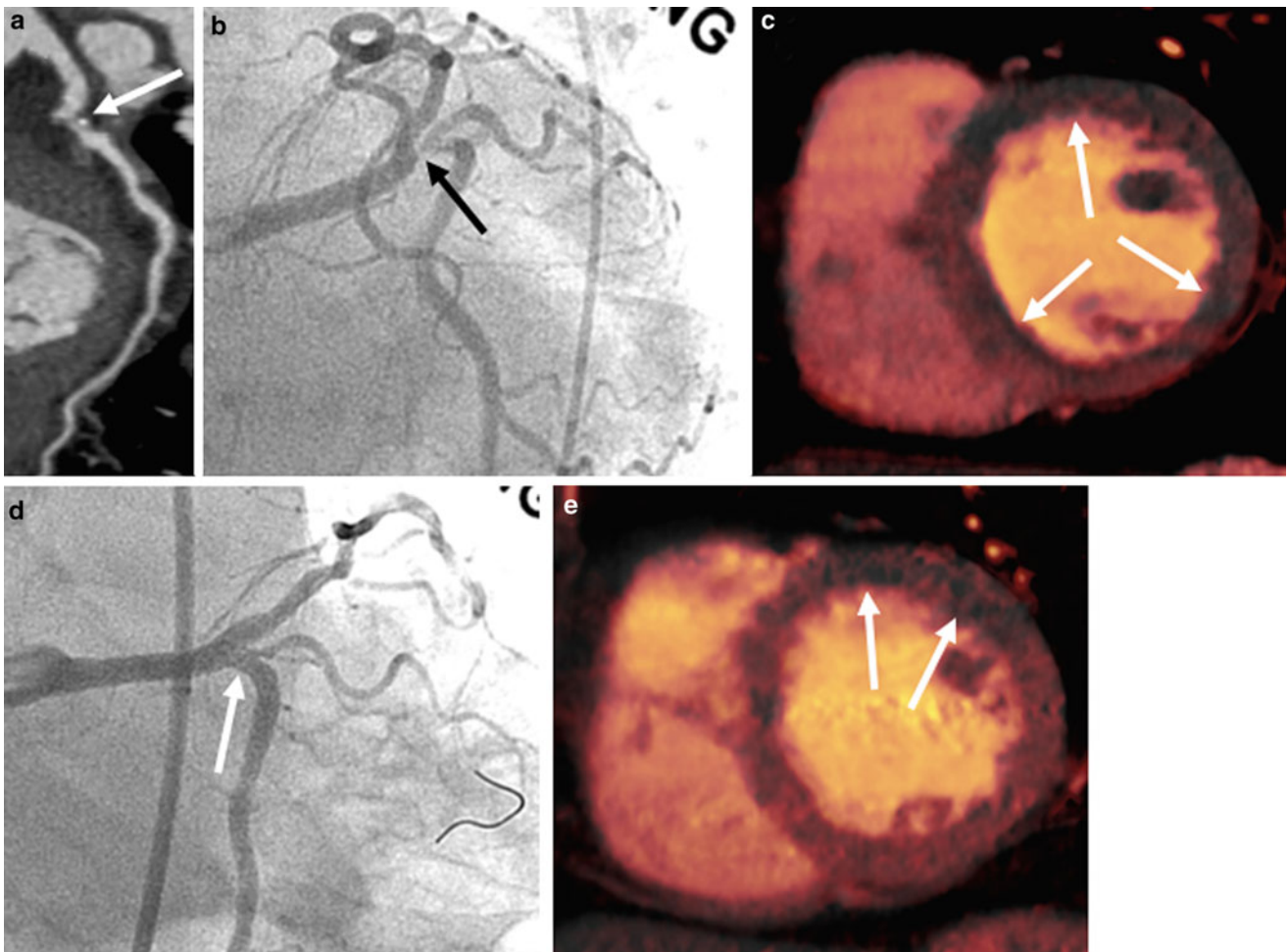


Fig. 15 Example of stress DECT perfusion for stent evaluation. Curved multiplanar reformatted coronary CT angiographic image (a) shows significant stenosis with mixed calcified and non-calcified plaques (arrow) in the ostium of the left circumflex artery (LCx). Conventional coronary angiogram finding (b) confirms the presence of significant stenosis (arrow) in LCx ostium. DECT-based iodine distribution mapping during adenosine infusion (c) reveals concentric blood pool deficits (arrows) in the mid LV myocardium. The patient

underwent percutaneous coronary intervention with stent implantation in the LCx ostium. Conventional coronary angiogram (d) shows restoration of the expected normal lumen diameter of LCx ostium (arrow). DECT-based iodine distribution map during adenosine infusion (e) reveals disappearance of previously noted blood pool deficits in the mid lateral, inferior, and inferoseptal LV myocardium but shows persistent blood pool deficits (arrows) in the mid anterior LV myocardium

perfusion with administration of pharmacologic stressors is more physiologically acceptable and feasible than DECT at rest in detecting reversible myocardial ischemia because adenosine increases the difference in myocardial perfusion between the ischemic and normally perfused myocardium. The rationale that an adenosine stress DECT-based iodine distribution map might be sensitive for the detection of hemodynamically significant stenosis causing a reversible myocardial perfusion deficit is supported by the advantages of the combined application of DECT and adenosine-induced stress CT perfusion imaging (Figs. 11, 12, 13, 14, 15). The clinical evidence supporting the accuracy and feasibility of stress DECT for the assessment of myocardial perfusion deficits comes from two published single-center

studies. Adenosine stress DECT perfusion was first evaluated in 41 patients with known CAD identified on CCTA, which were scheduled to undergo CCA. We demonstrated that stress DECT perfusion had a sensitivity, specificity, and accuracy of 89, 78, and 82 %, respectively, for the detection of myocardial segments with reversible perfusion deficits; adenosine stress cardiac MR perfusion, performed in 28 patients, was the gold standard for comparison. Compared with CCA, stress DECT perfusion had a sensitivity, specificity, and accuracy of 89, 78, and 82 %, respectively, for the detection of vascular territories with ischemic perfusion defects that were supplied by a vessel with ≥ 50 % stenosis on CCA (Ko et al. 2011). Most recently, we evaluated the incremental value of stress DECT perfusion in 45 patients

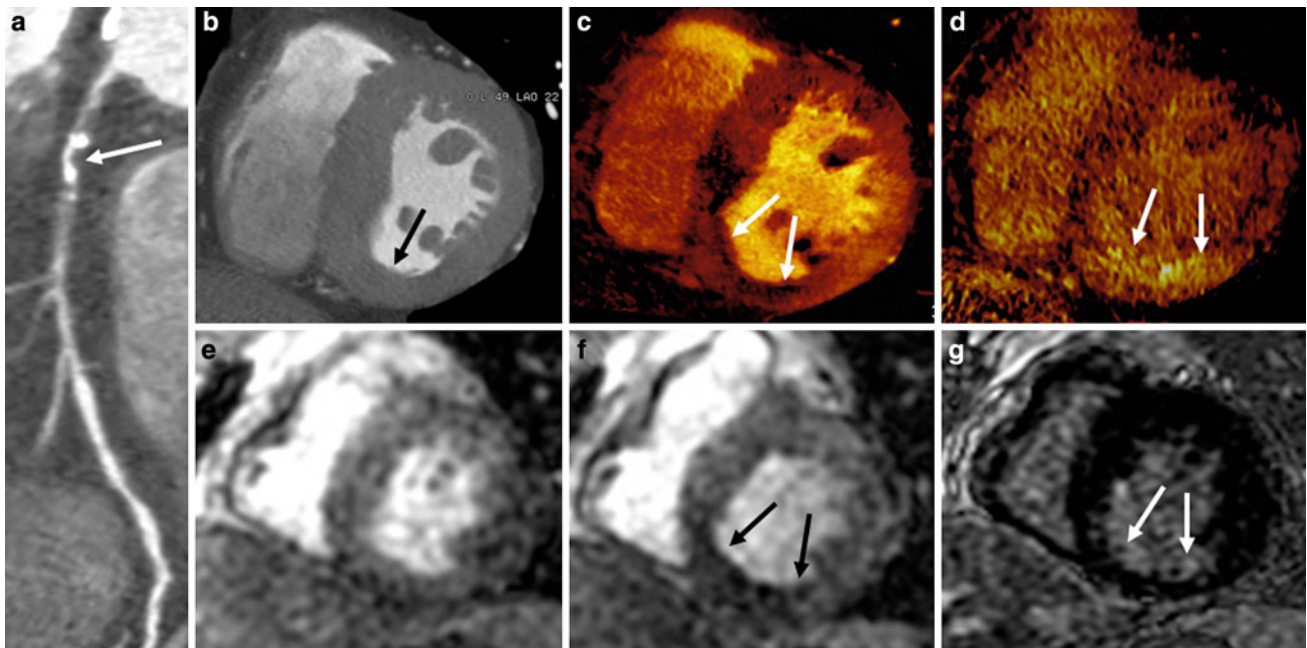


Fig. 16 Example of stress DECT perfusion identifying peri-infarct ischemia. Curved multiplanar reformatted coronary CT angiographic image (a) shows total occlusion with mixed calcified and non-calcified plaques (arrow) in the proximal segment of right coronary artery (RCA). The rest CT perfusion image (b) reveals thinned mid inferior left ventricular (LV) myocardium without perfusion deficit (arrow). DECT-based iodine distribution mapping during adenosine infusion

(c) reveals subendocardial blood pool deficits (arrows) in the mid inferior and inferoseptal LV myocardium. Delayed iodine uptake (arrows) representing myocardial infarction is noted on delayed-phase DECT (d). These findings (arrows) are in good correlation with rest (e) and stress (f) perfusion and delayed contrast-enhanced (g) cardiac MR images, corresponding to old subendocardial myocardial infarction with peri-infarct ischemia at RCA territory

with known CAD, confirmed on CCTA, who were scheduled for CCA (Ko et al. 2012a). We illustrated that the stress DECT perfusion, compared with CCA, had a sensitivity of 89 %, specificity of 74 %, PPV of 80 %, and NPV of 85 % for the detection of vascular territories with myocardial perfusion defects, supplied by significant coronary stenosis. Sensitivity, specificity, positive predictive value, and negative predictive value of the CCTA on a per-vessel basis, before stress DECT perfusion, were 92, 68, 74, and 88 %, respectively, and after stress DECT perfusion were 93, 86, 88, and 91 %, respectively, for the detection of significant coronary stenoses. We demonstrated that the combination of CCTA and stress DECT perfusion had incremental diagnostic value over CCTA alone for the detection of CAD (Ko et al. 2012a). These two studies can be summarized as follows: (1) stress DECT perfusion allows good diagnostic accuracy in detecting stress-induced myocardial perfusion deficits, as seen on stress cardiac MR perfusion, (2) that stress DECT perfusion plays a complementary role to enhance the diagnostic accuracy of CCTA for detecting CAD and (3) the clinical impact and the incremental value of DECT perfusion need to be evaluated in larger cohorts and multicenter studies.

7.3 Comparison Between Rest Dual-Energy CT and Stress Dual-Energy CT Perfusion Imaging

Both rest and stress DECT perfusion use a single acquisition of volume data during the first-pass enhancement phase for the assessment of myocardial blood volume distribution. Rest DECT is focused on the morphological and functional assessment of coronary stenoses during a single cardiac examination. However, stress DECT perfusion is primarily aimed to detect myocardial perfusion abnormalities (Fig. 16). Accordingly, contrast agent injection protocol needs to be modified for stress DECT perfusion imaging, while rest DECT uses the same protocol as routine CCTA.

The clinical evidence on utilizing iodine distribution maps for the assessment of myocardial blood-pool deficits has generally demonstrated good agreement between rest DECT perfusion and SPECT findings. More importantly, rest DECT perfusion has the potential to identify myocardial segments with stress induced ischemia, seen on SPECT. Accordingly, rest DECT has been considered to be a revolutionary tool for myocardial perfusion imaging, particularly in light of its utility for the detection of myocardial

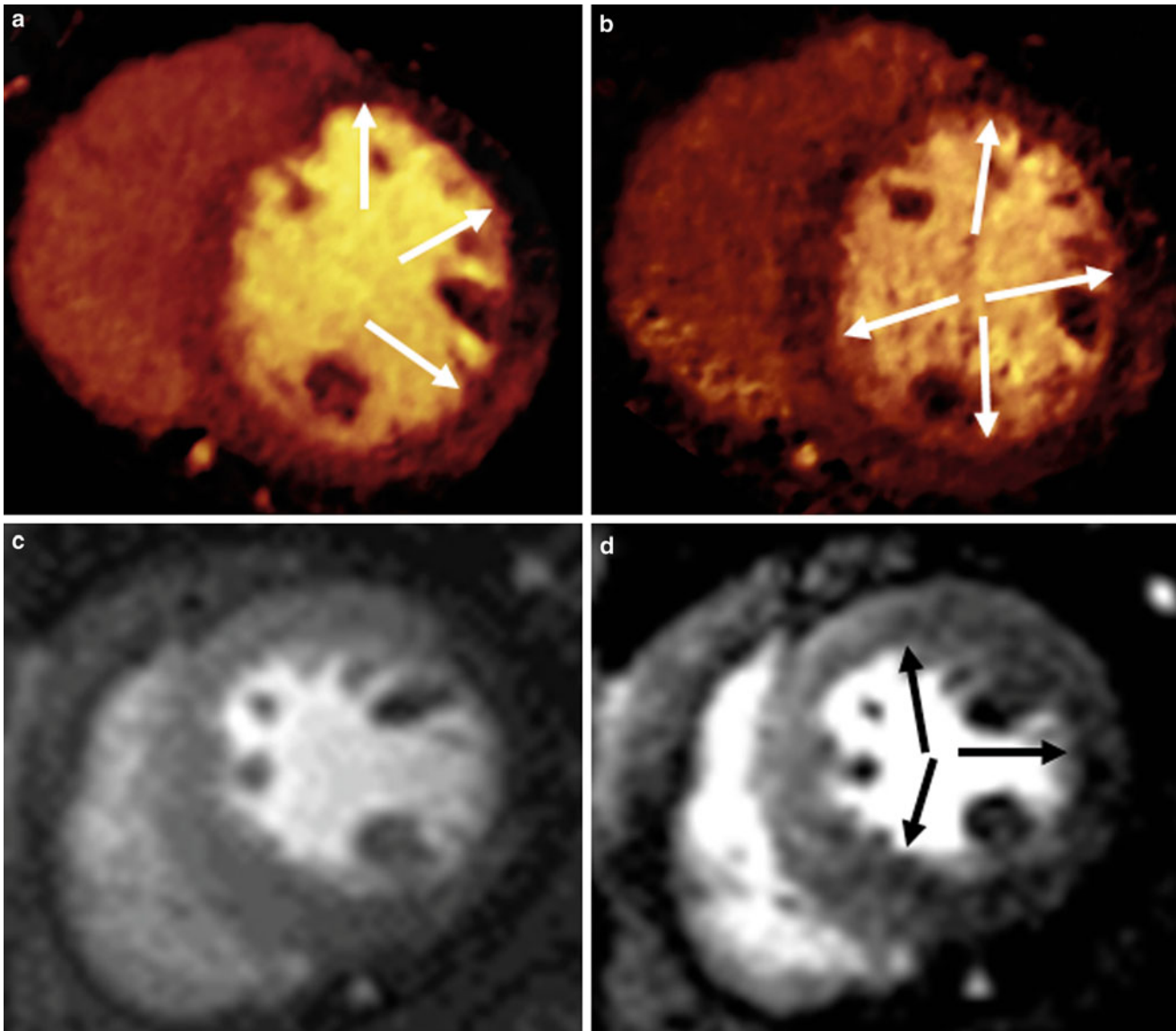


Fig. 17 Example of the superiority of stress DECT perfusion imaging when compared to rest DECT perfusion imaging identifying reversible perfusion defects. DECT-based iodine distribution maps at rest (**a**) shows blood pool deficits (*arrows*) in the mid anteroseptal, anterior, and lateral left ventricular (LV) myocardium. Stress DECT iodine distribution map (**b**) shows blood pool deficits (*arrows*) in the mid anterior, lateral, inferoseptal, and inferior LV myocardium. Rest (**c**) and stress (**d**) cardiac MR perfusion images reveal reversible

perfusion defects (*arrows*) in the mid anterior, lateral, inferoseptal, and inferior LV myocardium. Conventional coronary angiogram (not shown) reveals significant stenoses in the ostium of the left anterior descending coronary artery, first diagonal branch, first obtuse marginal branch, posterior descending coronary artery, and the posterolateral branch. Stress DECT perfusion is more sensitive for the detection of reversible myocardial blood pool deficits, than rest DECT perfusion

ischemia without the need for pharmacologic vasodilator agents. The combination of morphologic imaging of coronary arteries and functional imaging of myocardial perfusion may be a powerful non-invasive imaging method that provides comprehensive information, for CAD diagnosis and treatment planning. However, only a few studies are available to date and these have typically included too few patients. In addition, there has been a tendency for selection bias due to the specific recruitment of patients with

abnormal SPECT results, which leads to the overoptimistic assessment and false positives of rest DECT perfusion results. In addition, the mechanism of rest DECT perfusion for the detection of subtle differences in myocardial perfusion without the administration of a pharmacologic stressor needs to be more systematically investigated for clinical applications. Stress DECT perfusion might be more sensitive for the detection of myocardial blood pool deficits, especially reversible perfusion deficits, than rest DECT

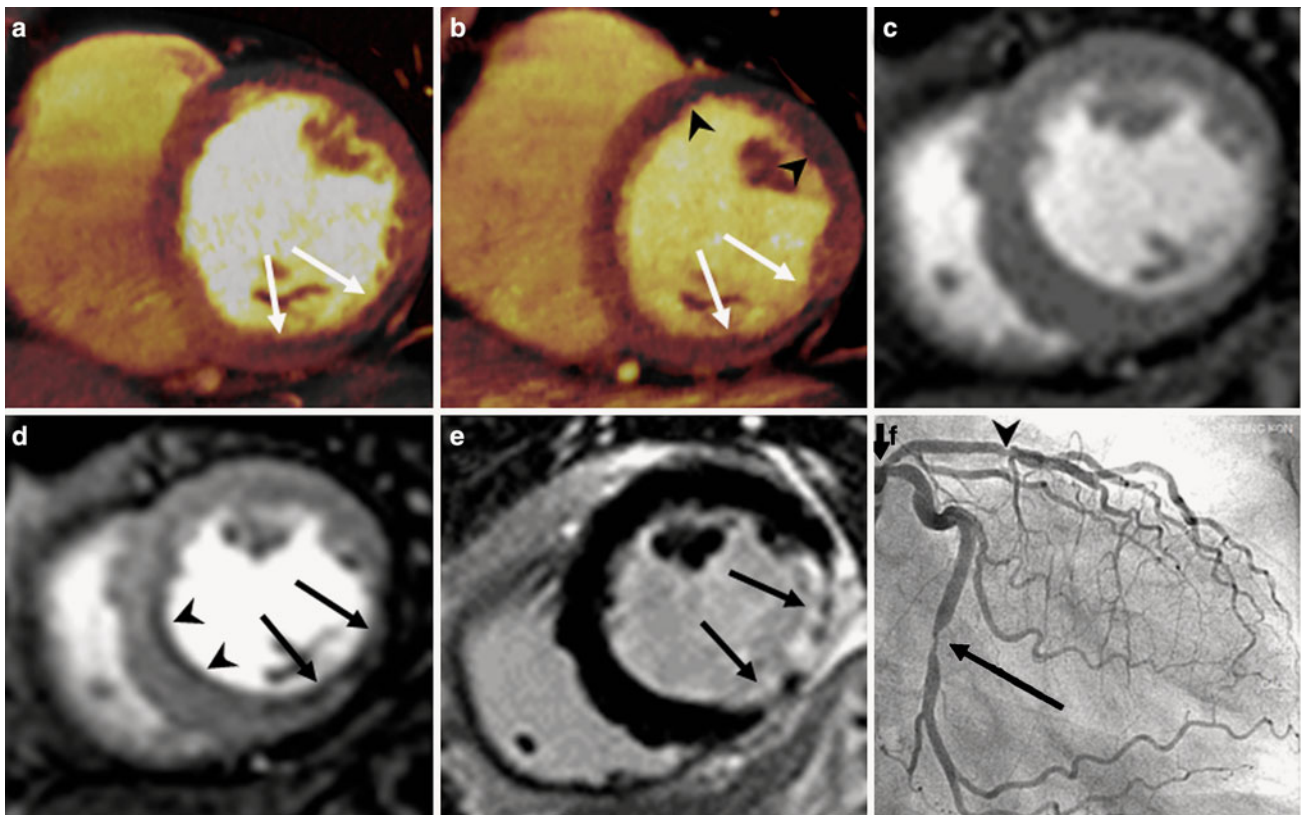


Fig. 18 Example of correlation among rest and stress DECT perfusion and cardiac MR. DECT-based iodine distribution maps at rest (a) and stress (b) show blood pool deficits (arrows) in the thinned mid inferolateral and inferior left ventricular (LV) myocardium. Rest (c) and stress (d) cardiac MR perfusion images reveal partially reversible subendocardial perfusion defects (arrows) at the corresponding left circumflex artery (LCx) territory. Delayed-phase cardiac MR image (e) shows delayed transmural hyperenhancement (arrows)

in the corresponding myocardium. Stress DECT iodine distribution map (b) reveals stress-induced blood pool deficits (arrowheads) in the mid anterior and anteroseptal LV myocardium. Reversible perfusion defect (arrowhead) is only noted in the mid anteroseptum of LV myocardium on rest (c) and stress (d) cardiac MR perfusion images. Conventional coronary angiogram (f) shows significant stenoses in the ostium (short arrow) and proximal segment (arrowhead) of the left anterior descending coronary artery and distal LCx (long arrow)

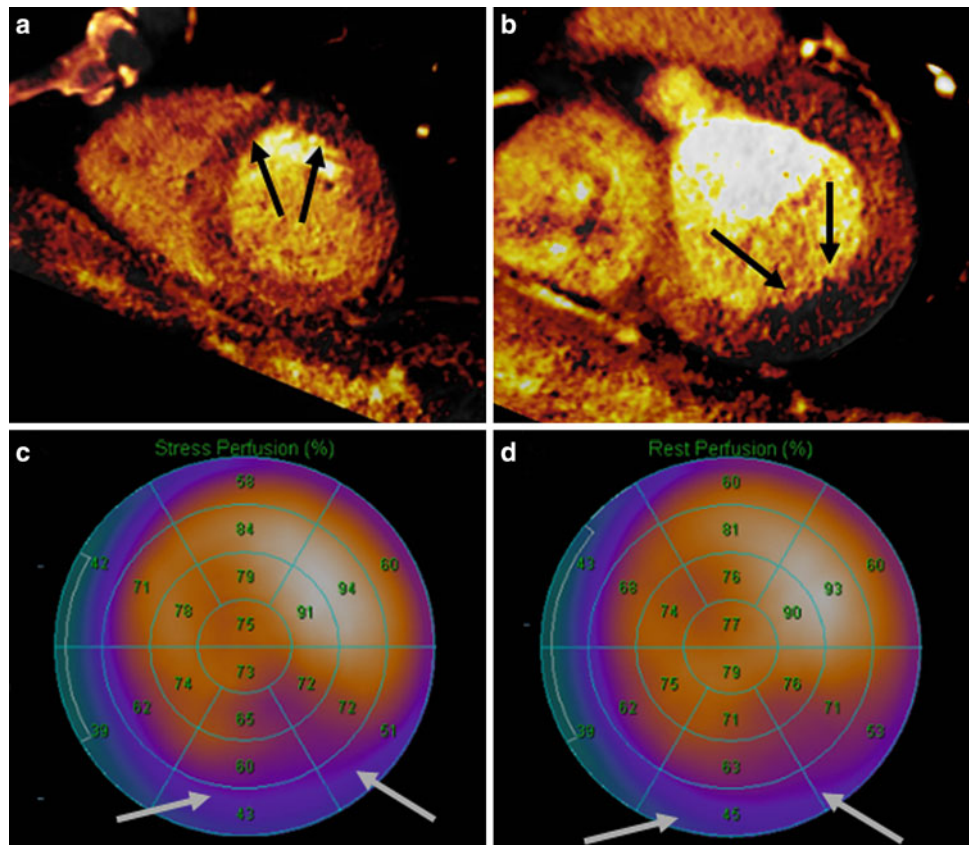
perfusion. Furthermore, stress DECT perfusion may be better at detecting small areas of myocardial ischemia and balanced myocardial ischemia in multivessel disease or microvascular disease, compared to rest DECT perfusion and SPECT (Figs. 14, 17). Although the results of clinical trials using stress DECT perfusion are promising, the published studies come from a single center and have included a limited number of patients. In addition, stress DECT perfusion is rather susceptible to cardiac motion artifacts, which degrade image quality and affect diagnostic accuracy for the detection of myocardial ischemia. Given the temporal resolution of 280 or 330 ms associated with the dual-source DECT, it is not feasible to accurately identify coronary stenoses with stress DECT. Thus, prospective studies with a direct comparison of rest DECT and stress DECT in the same patient are needed to systematically determine the exact performance of rest DECT and stress DECT, compared with the clinical reference standards, such as adenosine stress cardiac MR perfusion, SPECT or FFR. (Fig. 18)

8 Challenges, Pitfalls, and Limitations of Dual-Energy CT Perfusion

8.1 Radiation Dose

Patient's exposure to ionizing radiation is a major concern in DECT perfusion. Recent studies have demonstrated that rest DECT can be performed with radiation doses similar to the single-energy CCTA (mean of 12 mSv), using the conversion coefficient of $0.014 \text{ mSv} \cdot \text{mGy}^{-1} \text{ cm}^{-1}$ (Ruzsics et al. 2008, 2009; Wang et al. 2011; Hausleiter et al. 2009). DECT scans routinely rely on ECG-dependent tube current modulation, but cannot use prospective ECG-triggering or high-pitch factor ECG-synchronized spiral mode like single-energy CCTA or stress CT perfusion due to limitations of the contemporary dual-source CT in dual-voltage mode. However, rest DECT has significantly lower radiation dose compared with the combination of CCTA or CCA and SPECT. The average stress DECT perfusion effective

Fig. 19 Beam-hardening artifacts. Rest DECT iodine distribution maps (a, b) show blood pool deficits (arrows) in the apical anterior and septal (a) and basal inferolateral left ventricular (LV) myocardium (b). These lesions are not seen in the myocardial perfusion SPECT at stress (c) and rest (d). Fixed perfusion defects (arrows) seen on SPECT (c, d) are probably associated with attenuation artifacts in the basal inferior and inferolateral LV myocardium



radiation dose using 80/140 kV (5.8 mSv) was lower than that of single-energy CT perfusion (9.5 mSv) and SPECT under stress (9.2 mSv) in the recent study (Blankstein et al. 2009). The average effective radiation exposure for combined protocol of retrospective CCTA and stress DECT perfusion (14.5 mSv) was comparable with or even higher than combined single-energy prospective CCTA rest/stress CT protocol (12 mSv) and rest/stress SPECT (13 mSv) (Ko et al. 2011, 2012a; Blankstein et al. 2009). However, prospective ECG-gating permits radiation dose reductions for routine CCTA, allowing combined prospective CCTA/stress DECT perfusion to be performed with radiation doses comparable to or lower than rest/stress SPECT and combined single-energy CCTA/stress CT perfusion. Accordingly, stress DECT perfusion has the potential to become an attractive alternative to standard SPECT for the detection of myocardial ischemia, considering its relatively low radiation exposure, simple study protocol, short examination time, and high spatial resolution.

8.2 Artifacts

The recognition of differences in iodine concentration between ischemic myocardium and normally perfused myocardium is crucial in DECT perfusion. An iodine

distribution map contains a very broad range of iodine concentrations within the myocardium (normal variation in CT attenuation in different myocardial areas) and may be compromised by artifacts, such as beam hardening, cardiac motion, reconstruction, and misalignment. Normal LV myocardial enhancement, using a 320-slice MDCT coronary angiography, demonstrated that the lateral wall had significantly lower HU values when compared with the anterior, septal, and inferior walls in healthy patients without identified CAD (Crossett et al. 2011). Therefore, normal non-uniform attenuation values within the LV myocardium may be misinterpreted as perfusion defects on CT perfusion. Beam-hardening artifacts are commonly noted in CT perfusion and create focal areas of hypoattenuation in the myocardium, mainly seen in the LV basal inferior, apical anterior, and apical inferior walls (Figs. 19, 20). Beam hardening is caused by the selective absorption of low-energy photons by bony structures (spine, sternum, ribs), the contrast filled LV cavity, or the descending thoracic aorta (Rodriguez-Granillo et al. 2010; Mehra et al. 2011). DECT perfusion is prone to cardiac motion artifacts, particularly with the elevated heart rates required for the stress phase acquisition. In dual-energy mode, temporal resolution of dual-source CT is reduced, preventing freezing of cardiac motion as would be possible in single-energy mode, and thereby causing heart motion artifacts in DECT-

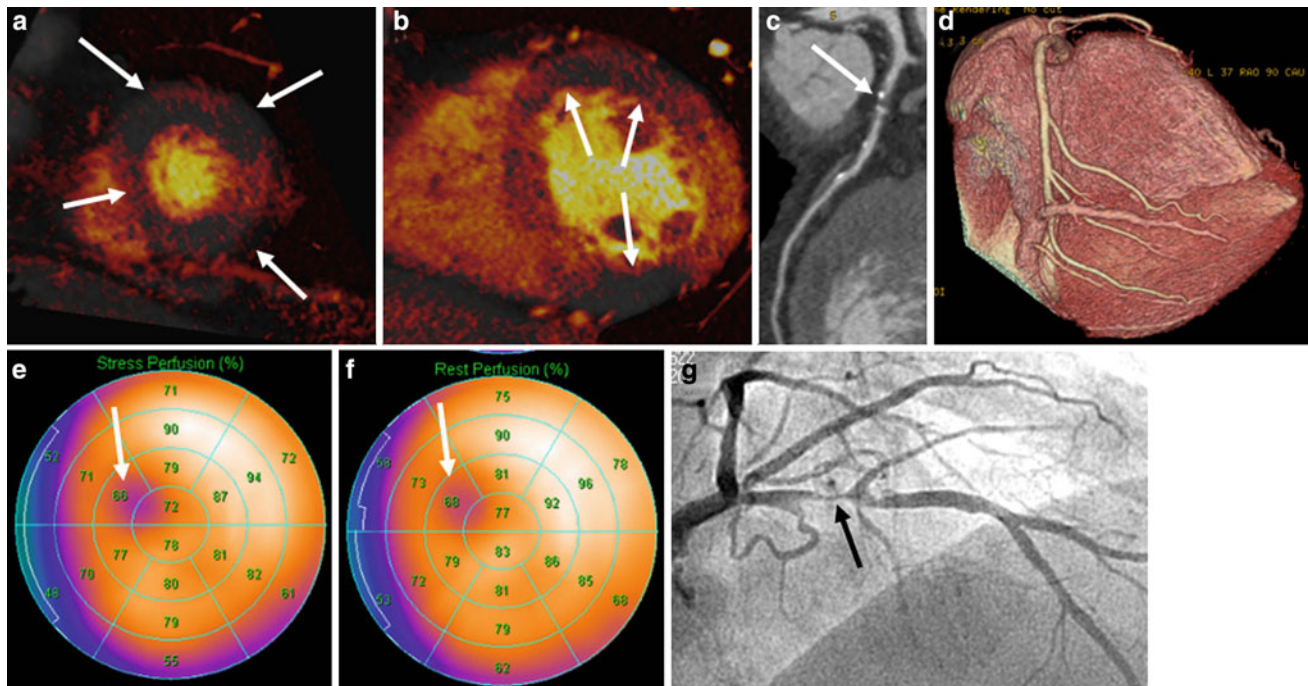


Fig. 20 Example of true and false positive rest DECT perfusion. DECT-based iodine distribution maps at rest (**a**, **b**) reveal blood pool deficits (*arrows*) in the apical to mid anterior and inferior and apical septum of left ventricular (LV) myocardium, corresponding to significant stenoses in the left anterior descending coronary artery (LAD) and the right coronary artery (RCA). Curved multiplanar reformatted coronary CT angiographic image (**c**) shows severe stenosis with mixed calcified and non-calcified plaques (*arrow*) in the proximal

segment of LAD. Three-dimensional volume-rendered reconstruction image (**d**) reveals right coronary dominance without stenoses in RCA branches. Myocardial perfusion SPECT at stress (**e**) and rest (**f**) show fixed perfusion defect (*arrows*) in the apical anteroseptum of LV myocardium. Conventional coronary angiogram (**g**) confirms the presence of severe stenosis in the proximal LAD (*arrow*). The false positive finding of DECT in the apical to mid inferior LV wall is related to the beam-hardening artifact

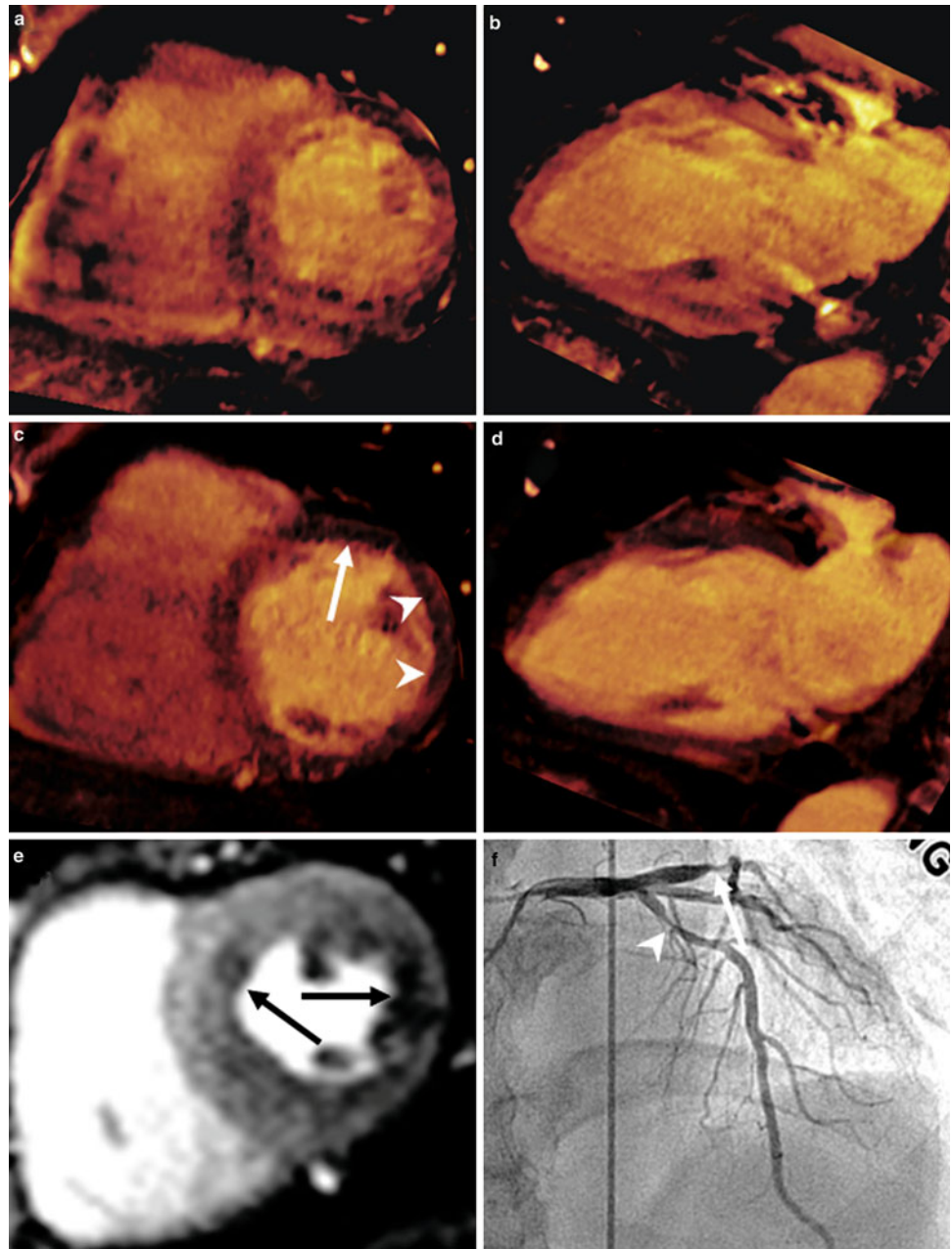
based myocardial iodine distribution maps (Ko et al. 2011, 2012a). Cardiac motion artifacts cause hypoenhanced or hyperenhanced areas that can mimic or mask perfusion defects (Fig. 21). Accordingly, stress DECT perfusion is not preferred in patients with high or irregular heart rates.

Multiphase evaluation helps to differentiate a true perfusion defect, an area of hypoattenuation that persists through all cardiac phases, from a cardiac motion artifact, which often disappears or changes location. Cone-beam artifact is the most common reconstruction artifact and presents as hypo- and hyperattenuation bands that most often affect the LV inferior wall. These artificial bands continue outside the cardiac silhouette across the entire field of view and can be differentiated from true perfusion defects, which are confined to the cardiac silhouette. Misalignment artifacts are based on the limited scan coverage of the dual-source DECT scanner, requiring the heart to be imaged over several heart beats. The temporal difference or non-uniformity in the cardiac position in any given heart beat gives rise to relative attenuation differences between the LV anterior and inferior walls (Mehra et al. 2011).

9 Summary and Conclusion

Contrast-enhanced rest DECT perfusion enables the evaluation of changes in the status of the myocardial blood supply. The rest DECT iodine distribution map makes hypoperfused myocardial areas more conspicuous and permits the identification of areas of reversible myocardial ischemia when compared with stress DECT results. Therefore, rest DECT has expanded the clinical application of MDCT as a “one-stop shop” imaging modality to identify both CAD and myocardial blood pool deficits in a single examination. Stress DECT perfusion has the potential to become a robust clinical tool for the detection of myocardial ischemia. The combined approach of CCTA and stress DECT perfusion allows identification of hemodynamically significant coronary lesions in high-risk patients with a large calcified plaque burden or stents, and thereby, provides useful information in assessing the need for CCA and revascularization procedures (Fig. 22). The radiation exposure for stress DECT perfusion is lower than stress

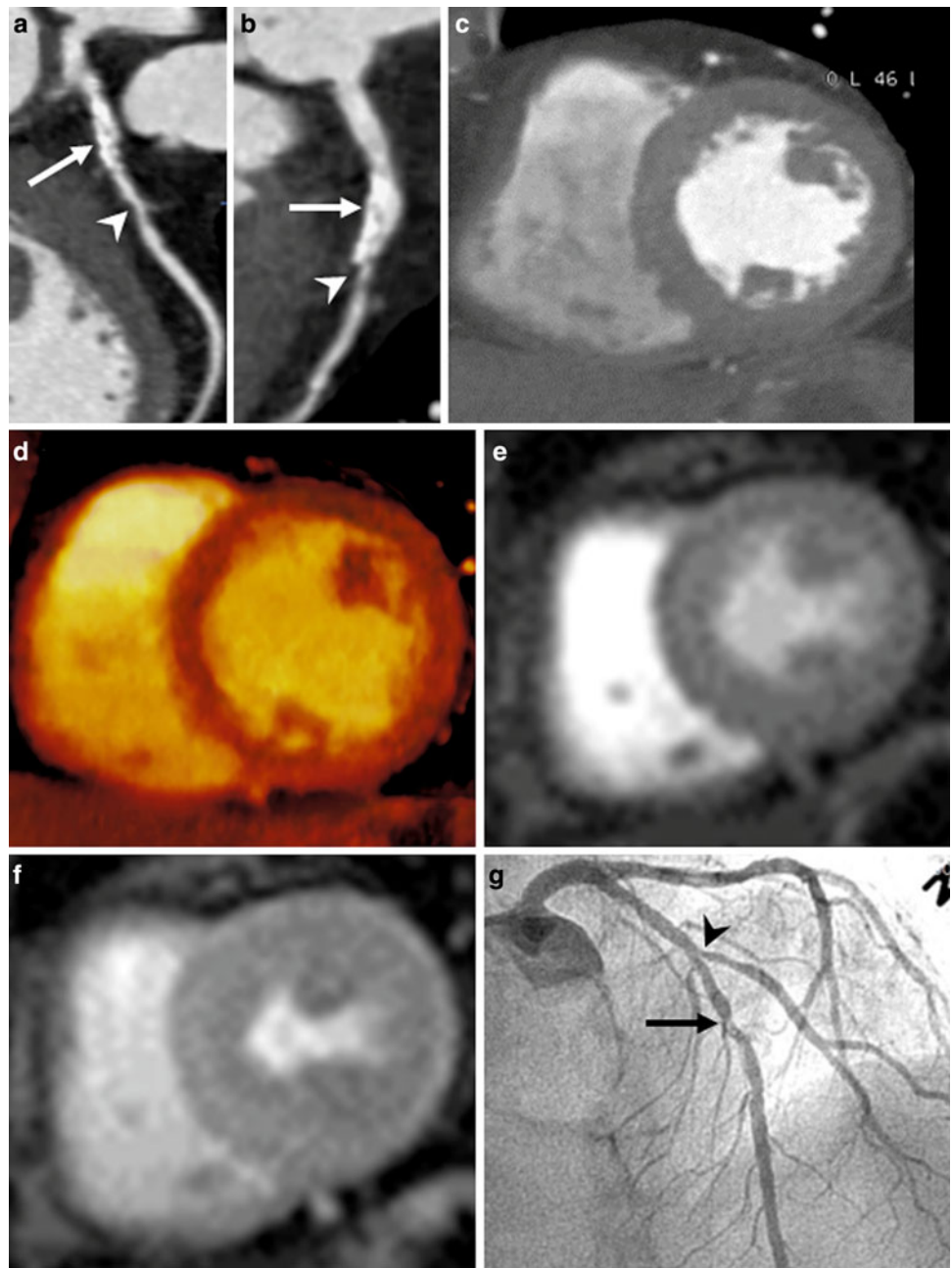
Fig. 21 Cardiac motion artifacts. Cardiac motion during image acquisition distorts the image and creates bands that appear to have reduced iodine uptake, possibly mimicking or masking myocardial blood pool deficits. Short axis (a) and two-chamber (b) views of stress DECT iodine distribution maps reveal severe cardiac motion artifacts due to a high heart rate (mean heart rate of 88 beats per minute), leading to inability to assess perfusion abnormalities. Short axis (c) and two-chamber (d) views of rest DECT iodine distribution maps show band-like blood pool deficits (arrow) in the mid anterior left ventricular (LV) myocardium, corresponding to cardiac motion artifact due to a heart rate of 78 beats per minute. Subendocardial blood pool deficit (arrowheads) is noted in the mid anterolateral LV myocardium on rest DECT iodine distribution map (c). Stress cardiac MR perfusion image (e) reveals stress-induced perfusion defects (arrows) in the mid-anteroseptal and mid-lateral LV myocardium. Conventional coronary angiogram (f) shows significant stenoses in the proximal segment of the left anterior descending coronary artery (arrow) and the left circumflex artery (arrowhead)



SPECT. Despite these promising results, however, stress DECT perfusion imaging is relatively less well known and less performed than a single-energy stress CT perfusion imaging. At present, most clinical data on DECT perfusion imaging are based on small diagnostic, single-center studies. Cardiac motion artifacts and beam hardening artifacts are major causes of false positive results when evaluating DECT-based myocardial iodine distribution maps for the detection of perfusion abnormalities. Diagnostic performance of rest DECT perfusion imaging needs to be validated with a direct comparison between the rest DECT and stress DECT perfusion by using adequate gold standards,

such as stress cardiac MR perfusion. Stress DECT perfusion requires technological advances and optimized acquisition and reconstruction protocols to enhance the diagnostic accuracy of CT perfusion with reduced radiation exposure to patients. In addition, the clinical impact and the incremental value of DECT perfusion need to be further evaluated in larger cohorts and multicenter studies. These efforts can promote the use of DECT perfusion in clinical practice. In conclusion, DECT of the heart is the promising complementary perfusion imaging technique in the diagnosis of CAD and has the potential to provide a new paradigm to the non-invasive assessment of CAD (Fig. 22).

Fig. 22 Combined approach of coronary CT angiography and stress DECT perfusion. Curved multiplanar reformatted coronary CT angiographic images (**a**, **b**) show heavily calcified plaque (*arrows*) in the proximal segment of the left anterior descending coronary artery (LAD) and significant stenoses (*arrowheads*) with non-calcified plaque in the middle LAD (**a**) and first diagonal branch (D1, **b**). Rest CT perfusion image (**c**) and stress dual-energy CT-based iodine distribution map (**d**) does not show blood pool deficits in the left ventricular (LV) myocardium. Rest (**e**) and stress (**f**) cardiac MR perfusion images confirm no stress inducible perfusion defects in the LV myocardium. Conventional coronary angiogram finding (**g**) confirms the presence of significant (75 % lumen reduction) stenosis in the ostium of D1 (*arrowhead*) and insignificant stenoses in proximal and middle LAD (*arrow*). The patient did not undergo percutaneous coronary intervention treatment for D1 stenosis because of the results of the DECT and cardiac MR perfusion studies



Acknowledgments The author sincerely thanks Dr. Meong Gun Song, Department of Thoracic Surgery at Konkuk University Medical Center, Dr. Tae-Hwan Lim, Department of Radiology at Asan Medical Center, Dr. Bernhard Krauss, Jungmin Hwang, and the CT technologists and the Radiology Department nursing staff at Konkuk University Medical Center.

References

- Arnoldi E, Lee YS, Ruzsics B et al (2011) CT detection of myocardial blood volume deficits: dual-energy CT compared with single-energy CT spectra. *J Cardiovasc Comput Tomogr* 5:421–429
- Bamberg F, Becker A, Schwarz F et al (2011) Detection of hemodynamically significant coronary artery stenosis: incremental diagnostic value of dynamic CT-based myocardial perfusion imaging. *Radiology* 260:689–698
- Blankstein R, Shturman LD, Rogers IS et al (2009) Adenosine-induced stress myocardial perfusion imaging using dual-source cardiac computed tomography. *J Am Coll Cardiol* 54:1072–1084
- Chandrasekar B, Doucet S, Bilodeau L et al (2001) Complications of cardiac catheterization in the current era: a single-center experience. *Catheter Cardiovasc Interv* 52:289–295
- Chiro GD, Brooks RA, Kessler RM et al (1979) Tissue signatures with dual-energy computed tomography. *Radiology* 131:521–523
- Crossett MP, Schneider-Kolsky M, Troupis J (2011) Normal perfusion of the left ventricular myocardium using 320 MDCT. *J Cardiovasc Comput Tomogr* 5:406–411

- Flohr TG, McCollough C, Bruder H et al (2006) First performance evaluation of a dual source CT (DSCT) system. *Eur Radiol* 16:256–268
- Gaemperli O, Schepis T, Valenta I et al (2007) Cardiac image fusion from stand-alone SPECT and CT: clinical experience. *J Nucl Med* 48:696–703
- Gaemperli O, Schepis T, Valenta I et al (2008) Functionally relevant coronary artery disease: comparison of 64-section CT angiography with myocardial perfusion SPECT. *Radiology* 248:414–423
- George RT, Silva C, Cordeiro MA et al (2006) Multidetector computed tomography myocardial perfusion imaging during adenosine stress. *J Am Coll Cardiol* 48:153–160
- George RT, Jerosch-Herold M, Silva C et al (2007) Quantification of myocardial perfusion using dynamic 64-detector computed tomography. *Invest Radiol* 42:815–822
- Hachamovitch R, Berman DS, Kiat H et al (1996) Exercise myocardial perfusion SPECT in patients without known coronary artery disease: incremental prognostic value and use in risk stratification. *Circulation* 93:905–914
- Hausleiter J, Meyer T, Hermann F et al (2009) Estimated radiation dose associated with cardiac CT angiography. *JAMA* 301:500–507
- Heller GV, Calnon D, Dorbala S (2009) Recent advances in cardiac PET and PET/CT myocardial perfusion imaging. *J Nucl Cardiol* 16:962–969
- Johnson TR, Krauss B, Sedlmair M et al (2007) Material differentiation by dual energy CT: initial experience. *Eur Radiol* 17:1510–1517
- Kang DK, Schoepf UJ, Bastarrika G, Nance JW, Abro JA, Ruzsics B (2010) Dual-energy computed tomography for integrative imaging of coronary artery disease: principles and clinical applications. *Semin Ultrasound CT MRI* 31:276–291
- Ko SM, Choi JW, Song MG et al (2011) Myocardial perfusion imaging using adenosine-induced stress dual-energy computed tomography of the heart: comparison with cardiac magnetic resonance imaging and conventional coronary angiography. *Eur Radiol* 21:26–35
- Ko SM, Choi JW, Hwang HK et al (2012a) Diagnostic performance of combined noninvasive anatomic and functional assessment with dual-source CT and adenosine-induced stress dual-energy CT for detection of significant coronary stenosis. *Am J Roentgenol* 98:512–520
- Ko BS, Cameron JD, Meredith IT et al (2012b) Computed tomography stress myocardial perfusion imaging in patients considered for revascularization: a comparison with fractional flow reserve. *Eur Heart J* 33:67–77
- Mehra V, Valdiviezo C, Arbab-zadeh A et al (2011) A stepwise approach to the visual interpretation of CT-based myocardial perfusion. *J Cardiovasc Comput Tomogr* 5:357–369
- Meijboom WB, van Mieghem CA, van Pelt N et al (2008) Comprehensive assessment of coronary artery stenoses. Computed tomography coronary angiography versus conventional coronary angiography and correlation with fractional flow reserve in patients with stable angina. *J Am Coll Cardiol* 52:636–643
- Millner MR, McDavid WD, Waggner RG, Dennis MJ, Payne WH, Sank VJ (1979) Extraction of information from CT scans at different energies. *Med Phys* 6:70–71
- Mühlenbruch G, Seyfarth T, Soo CS, Pregalathan N, Mahnken AH (2007) Diagnostic value of 64-slice multi-detector row cardiac CTA in symptomatic patients. *Eur Radiol* 17:603–609
- Nandalur KR, Dwamena BA, Choudhri AF, Nandalur MR, Carlos RC (2007) Diagnostic performance of stress cardiac magnetic resonance imaging in the detection of coronary artery disease: a meta-analysis. *J Am Coll Cardiol* 50:1343–1353
- Petersilka M, Bruder H, Krauss B, Stierstorfer K, Flohr TG (2008) Technical principles of dual source CT. *Eur J Radiol* 68:362–368
- Rocha-Filho JA, Blankstein R, Shturman LD et al (2010) Incremental value of adenosine-induced stress myocardial perfusion imaging with dual-source CT at cardiac CT angiography. *Radiology* 254:410–419
- Rodriguez-Granillo GA, Rosales MA, Degrossi E, Rodriguez AE (2010) Signal density of left ventricular myocardial segments and impact of beam hardening artifact: implications for myocardial perfusion assessment by multidetector CT coronary angiography. *Int J Cardiovasc Imaging* 26:345–354
- Ruzsics B, Lee H, Zwerner PL, Gebregziabher M, Costello P, Schoepf UJ (2008) Dual-energy CT of the heart for diagnosing coronary artery stenosis and myocardial ischemia-initial experience. *Eur Radiol* 18:2414–2424
- Ruzsics B, Schwarz F, Schoepf UJ et al (2009) Comparison of dual-energy computed tomography of the heart with single photon emission computed tomography for assessment of coronary artery stenosis and of the myocardial blood supply. *Am J Cardiol* 104:318–326
- Santana CA, Garcia EV, Faber TL et al (2009) Diagnostic performance of fusion of myocardial perfusion imaging (MPI) and computed tomography coronary angiography. *J Nucl Cardiol* 16:201–211
- Schwarz F, Ruzsics B, Schoepf UJ et al (2008) Dual-energy CT of the heart-principles and protocols. *Eur J Radiol* 68:423–433
- Vanhoeacker PK, Heijnenbrok-Kal MH, Van Heste R et al (2007) Diagnostic performance of multidetector CT angiography for assessment of coronary artery disease: meta-analysis. *Radiology* 244:419–428
- Vlahos I, Godoy MC, Naidich DP (2010) Dual-energy computed tomography imaging of the aorta. *J Thorac Imaging* 25:289–300
- Wang R, Yu W, Wang Y et al (2011) Incremental value of dual-energy CT to coronary CT angiography for the detection of significant coronary stenosis: comparison with quantitative coronary angiography and single photon emission computed tomography. *Int J Cardiovasc Imaging* 27:647–656
- Watkins S, McGeoch R, Lyne J et al (2009) Validation of magnetic resonance myocardial perfusion imaging with fractional flow reserve for the detection of significant coronary heart disease. *Circulation* 120:2207–2213